Acta Crystallographica Section B
Structural Science
ISSN 0108-7681

Correlation of structural and physico-chemical parameters with the bioactivity of alkylated derivatives of indole-3-acetic acid, a phytohormone (auxin)

Biljana Nigović,[a,b] Snježana Antolić,[a] Biserka Kojić-Prodić,[a]* Rudolf Kiralj,[a] Volker Magnus[a] and Branka Salopek-Sondi[a]

[a]Rudjer Bošković Institute, POB 1016, 10001 Zagreb, Croatia, and [b]Faculty of Pharmacy and Biochemistry, University of Zagreb, A. Kovačića 1, 10001 Zagreb, Croatia

Correspondence e-mail: kojic@rudjer.irb.hr

Received 17 December 1998
Accepted 4 May 1999

As part of molecular recognition studies on the phytohormone indole-3-acetic acid (IAA) a series of alkylated IAAs has been examined. Phenyl-ring substitution (alkyl = methyl and ethyl) at positions 4-, 6- or 7- as well as pyrrole substitution at the 2-site resulted in the six compounds which are analyzed: 2-Me-IAA, 4-Me-IAA, 6-Me-IAA, 7-Me-IAA, 4-Et-IAA and 6-Et-IAA. The structure–activity relationships investigated include those between the geometrical parameters of the molecular structures determined by X-ray analysis, the growth-promoting activities in the *Avena* coleoptile straight-growth bioassay and relative lipophilicities calculated from retention times on a reversed-phase HPLC column and from R_F values in reversed-phase TLC. Lipophilicities are correlated with the moments of inertia, average polarizability, molecular mass, and the van der Waals radii of the ring substituents. The influence of substitution on the electronic properties of the indole ring and its geometry is discussed on the basis of the UV and ^{1}H NMR spectra.

1. Introduction

Structure–activity correlations for the plant hormone (auxin), indole-3-acetic acid (IAA) and a number of its derivatives have attracted much attention over the last three decades (Tomić, Gabdoulline *et al.*, 1998, and references therein; Bandurski *et al.*, 1995; Libbenga *et al.*, 1986) with the goal of understanding the mechanism of the physiological effects at the molecular level, and of finding growth regulators and herbicides suitable for agricultural application. The biological activity of such compounds has been correlated with lipophilicity, electron and charge distribution in the aromatic ring systems, and stereochemistry (Hansch *et al.*, 1963; Thimann, 1977; Farrimond *et al.*, 1978; Schneider & Wightman, 1978; Katekar, 1979; Ramek *et al.*, 1995, 1996). No simple correlations of either physico-chemical properties or structural parameters with bioactivity have so far been found for indole-3-acetic acid derivatives. To understand the essential molecular properties of a substrate or an inhibitor for interaction with the auxin binding protein (ABP), the putative receptor (Barbier-Brygoo, 1995), the three-dimensional structure of this protein is required. This research is in progress (Klämbt, 1990; Tian *et al.*, 1995; Venis & Napier, 1995) and when the topology of the hormone-interactive site of ABP is known, complete structural data for a variety of substrates or inhibitors will be needed. A systematic classification of a set of ~50 compounds by interaction property-similarity indices was performed to distinguish auxins from inactive compounds

(Tomić, Gabdoulline *et al.*, 1998). This computational approach based on molecular properties can also be used to predict the activities of new plant growth substances and herbicides. To provide more data on potential auxins and non-auxins we have systematically studied monochlorinated (Nigović *et al.*, 1996) and dichlorinated IAAs (Antolić *et al.*, 1999), monofluorinated (Antolić *et al.*, 1996) and also *n*-alkylated IAAs (alkyl = Me, Et, Pr^n, Bu^n substituted at position 5 of IAA; Kojić-Prodić *et al.*, 1991). This paper is focused on the quantitative structure–property relationships of alkylated IAAs [alkyl = Me and Et, (1)]. The effect of substitution on the electronic properties of the indole aromatic system is examined on the basis of UV spectra and ^{1}H NMR data for IAA and its derivatives. The analysis includes the X-ray structures of six novel compounds, their growth-promoting activity using the *Avena* coleoptile straight-growth test, and their experimentally determined and calculated lipophilicities. In addition to the alkylated IAAs, the analysis also includes halogenated IAAs for comparison. The lipophilicity of the molecules studied is correlated with their average polarizabilities, their principal moments of inertia along the inertial axes, their relative molecular masses and the van der Waals radii of the substituents attached to the indole ring, using quantitative structure–property relationships (QSPR) methods [multiple linear regression (MLR), principal component analysis (PCA) and principal component regression (PCR)].

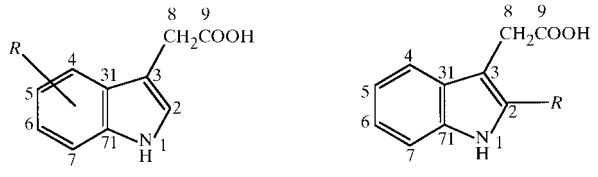

4-, 6-, 7-Me-IAA $R = -CH_3$
4-, 6-Et-IAA $R = -C_2H_5$

2-Me-IAA $R = -CH_3$

(I)

2. Experimental

2.1. Chemicals

IAA and 2-Me-IAA were obtained commercially. 5-Me-IAA, 5-Et-IAA, 5-Pr^n-IAA and 5-Bu^n-IAA (Ilić *et al.*, 1991) as well as 4-Et-IAA and 6-Et-IAA (Reinecke *et al.*, 1999) were prepared by Fischer cyclization of the corresponding ring-substituted phenylhydrazones. 4-Me-IAA (Thomson *et al.*, 1988), 6-Me-IAA and 7-Me-IAA (Stevens & Su, 1962) were synthesized from the respective methylindoles *via* the corresponding gramines, as described in detail for the 4-isomer (Reinecke *et al.*, 1999). In addition to the spectroscopic and X-ray diffraction data reported below, 6-Me-IAA was also characterized by melting point (430–431 K) and its exact molecular mass (189.0780 amu, while $C_{11}H_{11}NO_2$ requires 189.0790 amu), as determined by electron impact mass spectroscopy. 7-Me-IAA prepared by our method melted at 457–458 K (Stevens & Su, 1962, reported 454.5–456 K) and showed a molecular mass of 189.0782 amu.

2.2. X-ray measurements and structure determination

Crystals suitable for X-ray structure analysis were prepared by slow evaporation of 2 ml solutions containing 10–15 mg ml^{-1} of compounds in the following solvent mixtures: ethyl acetate and benzene (1:1 vol.) for 2-Me-IAA, acetone and chloroform (1:1 vol.) for 4-Me-IAA, acetone and dichloromethane (1:3 vol.) for 6-Me-IAA and 7-Me-IAA (1:2 vol.), cyclohexane and dichloromethane (1:3 vol.) for 4-Et-IAA, and acetone and *n*-hexane and chloroform (1:1:1, vol.) for 6-Et-IAA. An attempt to grow better quality crystals of 6-Et-IAA failed; they crystallized as thin plates. The crystals were grown at room temperature over 1–4 d. Relatively short crystallization times, adjusted by selection of solvents, were essential to prevent degradation of the compounds, which are also light sensitive. The crystals were achiral and they crystallized in $P2_1/c$ (and its equivalents) or *Pbca* (a single example, 6-Me-IAA). Data were collected on an Enraf–Nonius CAD-4 diffractometer (Tables 1 and 2) with graphite-monochromated Mo $K\alpha$ radiation in the dark. Lorentz and polarization corrections were applied using the Enraf–Nonius *SDP/VAX* package (B. A. Frenz & Associates Inc., 1982). The absorption and extinction corrections were not applied. Structures were solved by direct methods using the program *SHELXS*86 (Sheldrick, 1985) and refined by *SHELX*76 (Sheldrick, 1976) with a full-matrix least-squares procedure minimizing $\Sigma w(|F_o| - |F_c|)^2$ on F values. The non-H atoms were refined anisotropically. For 6-Et-IAA the diffraction data were poor because of the poor crystal quality; the structure was solved and refined, and although the bond lengths and angles are not good enough for comparisons, the conformation and packing are useful and have been included here. For the remaining structures difference Fourier maps were used to locate the H atoms and their coordinates were refined. The H atoms of the methyl groups were calculated on stereochemical grounds and refined riding on their respective C atoms. Details of the refinement procedures are listed in Tables 1 and 2. Scattering factors are those included in *SHELX*76 (Sheldrick, 1976). Molecular geometry was calculated by the program package *PLATON* (Spek, 1993). Drawings were prepared by the *PLUTON* program incorporated into *PLATON* and *ORTEP*II (Johnson, 1976). The final atomic coordinates and equivalent isotropic thermal parameters are listed in Tables 3–8.[1] Calculations were performed on an INDIGO-2 workstation at the Laboratory for Chemical Crystallography and Biocrystallography, Rudjer Bošković Institute, Zagreb, Croatia.

2.3. Computational methods

The geometries of indole-3-acetic acid and its 13 derivatives (Me-IAAs, F-IAAs and Cl-IAAs, including their positional

[1] Supplementary data for this paper are available from the IUCr electronic archives (Reference: HA0181). Services for accessing these data are described at the back of the journal.

Table 1
Experimental details.

	2-Me-IAA	4-Me-IAA	6-Me-IAA	7-Me-IAA	4-Et-IAA
Crystal data					
Chemical formula	$C_{11}H_{11}NO_2$	$C_{11}H_{11}NO_2$	$C_{11}H_{11}NO_2$	$C_{11}H_{11}NO_2$	$C_{12}H_{13}NO_2$
Chemical formula weight	189.21	189.21	189.21	189.21	203.24
Cell setting	Monoclinic	Monoclinic	Orthorhombic	Monoclinic	Monoclinic
Space group	$P2_1/c$	$P2_1/n$	$Pbca$	$P2_1/c$	$P2_1/n$
a (Å)	8.542 (1)	8.680 (1)	6.216 (1)	19.353 (1)	9.288 (1)
b (Å)	13.408 (1)	7.624 (1)	38.627 (1)	5.074 (1)	7.440 (1)
c (Å)	8.638 (1)	15.044 (1)	8.031 (1)	10.275 (1)	14.776 (1)
β (°)	99.70 (1)	101.87 (1)	90	109.00 (1)	103.53 (1)
V (Å^3)	975.18 (8)	974.27 (8)	1928.29 (18)	954.00 (9)	992.72 (8)
Z	4	4	8	4	4
D_x (Mg m^{-3})	1.289	1.290	1.304	1.317	1.360
Radiation type	Mo $K\alpha$	Mo $K\alpha$	Mo $K\alpha$	Mo $K\alpha$	Mo $K\alpha$
Wavelength (Å)	0.71073	0.71073	0.71073	0.71073	0.71073
No. of reflections for cell parameters	25	25	25	25	25
θ range (°)	7–18	6–18	6–17	6–17	6–18
μ (mm^{-1})	0.0964	0.0964	0.0974	0.0985	1.003
Temperature (K)	297	103	297	297	297
Crystal form	Prismatic	Prismatic	Prismatic	Prismatic	Plate
Crystal size (mm)	0.4 × 0.15 × 0.15	0.5 × 0.25 × 0.2	0.5 × 0.4 × 0.4	0.4 × 0.3 × 0.1	0.45 × 0.2 × 0.06
Crystal colour	Colourless	Colourless	Colourless	Colorless	Colourless
Data collection					
Diffractometer	Enraf–Nonius CAD-4	Enraf–Nonius CAD-4	Enraf–Nonius CAD-4	Enraf–Nonius CAD-4	Enraf–Nonius CAD-4
Data collection method	$\omega/2\theta$ scans	$\omega/2\theta$ scans	$\omega/2\theta$ scans	$\omega/2\theta$ scans	$\omega/2\theta$ scans
Absorption correction	None	None	None	None	None
No. of measured reflections	1920	1974	2040	1988	2594
No. of independent reflections	1467	1619	1398	1461	1526
No. of observed reflections	1052	1434	970	1038	999
Criterion for observed reflections	$I > 3\sigma(I)$	$I > 3\sigma(I)$	$I > 3\sigma(I)$	$I > 3\sigma(I)$	$I > 3\sigma(I)$
R_{int}	0.013	0.040	0.050	0.013	0.018
θ_{max} (°)	25	25	25	25	25
Range of h, k, l	$0 \rightarrow h \rightarrow 10$ $0 \rightarrow k \rightarrow 15$ $-10 \rightarrow l \rightarrow 10$	$0 \rightarrow h \rightarrow 10$ $0 \rightarrow k \rightarrow 9$ $-17 \rightarrow l \rightarrow 17$	$0 \rightarrow h \rightarrow 7$ $0 \rightarrow k \rightarrow 46$ $0 \rightarrow l \rightarrow 9$	$-22 \rightarrow h \rightarrow 21$ $0 \rightarrow k \rightarrow 6$ $0 \rightarrow l \rightarrow 12$	$-1 \rightarrow h \rightarrow 11$ $-1 \rightarrow k \rightarrow 8$ $-17 \rightarrow l \rightarrow 17$
No. of standard reflections	3	3	3	3	3
Frequency of standard reflections	Every 87 reflections	Every 87 reflections	Every 87 reflections	Every 87 reflections	Every 87 reflections
Intensity decay (%)	0.3	0.5	1.8	0.1	1.5
Refinement					
Refinement on	F	F	F	F	F
R	0.039	0.035	0.049	0.041	0.042
wR	0.043	0.041	0.041	0.036	0.046
S	0.39	0.41	0.99	0.47	0.62
No. of reflections used in refinement	1052	1434	970	1038	999
No. of parameters used	168	172	158	172	188
H-atom treatment	All H-atom parameters refined except U_{iso} for H101, H102, H103	All H-atom parameters refined except H1, H11 normalized	All H-atom parameters refined, except H101, H102, H103 parameters constrained, H1 normalized, H81, H82 riding	All H-atom parameters refined, except H1, H11 normalized	All H-atom parameters refined
Weighting scheme	$w = 1.478/[\sigma^2(F_o) + 0.001075(F_o^2)]$	$w = 1.456/[\sigma^2(F_o) + 0.001021(F_o^2)]$	$w = 3.731/\sigma^2(F_o)$	$w = 2.624/\sigma^2(F_o)$	$w = 0.849/[\sigma^2(F_o) + 0.002474(F_o^2)]$
$(\Delta/\sigma)_{max}$	0.05	0.005	0.05	0.05	0.01

Table 1 (continued)

	2-Me-IAA	4-Me-IAA	6-Me-IAA	7-Me-IAA	4-Et-IAA
$\Delta\rho_{max}$ (e Å^{-3})	0.17	0.23	0.16	0.14	0.019
$\Delta\rho_{min}$ (e Å^{-3})	−0.18	−0.24	−0.19	−0.15	−0.018
Extinction method	None	None	None	None	None
Source of atomic scattering factors	*International Tables for Crystallography* (1992, Vol. C, Tables 4.2.6.8 and 6.1.1.4)	*International Tables for Crystallography* (1992, Vol. C, Tables 4.2.6.8 and 6.1.1.4)	*International Tables for Crystallography* (1992, Vol. C, Tables 4.2.6.8 and 6.1.1.4)	*International Tables for Crystallography* (1992, Vol. C, Tables 4.2.6.8 and 6.1.1.4)	*International Tables for Crystallography* (1992, Vol. C, Tables 4.2.6.8 and 6.1.1.4)
Computer programs					
Data collection	*CAD*-4 (Enraf–Nonius, 1988)	*CAD*-4 (Enraf–Nonius, 1988)	*CAD*-4 (Enraf–Nonius, 1988)	*CAD*-4 (Enraf–Nonius, 1988)	*CAD*-4 (Enraf–Nonius, 1988)
Cell refinement	*CAD*-4 ⟨*CELDIM*⟩ routine	*CAD*-4 ⟨*CELDIM*⟩ routine	*CAD*-4 ⟨*CELDIM*⟩ routine	*CAD*-4 ⟨*CELDIM*⟩ routine	*CAD*-4 ⟨*CELDIM*⟩ routine
Data reduction	*SDP* (B. A. Frenz & Associates Inc., 1982)	*SDP* (B. A. Frenz & Associates Inc., 1982)	*SDP* (B. A. Frenz & Associates Inc., 1982)	*SDP* (B. A. Frenz & Associates Inc., 1982)	*SDP* (B. A. Frenz & Associates Inc., 1982)
Structure solution	*SHELXS*86 (Sheldrick, 1985)	*SHELXS*86 (Sheldrick, 1985)	*SHELXS*86 (Sheldrick, 1985)	*SHELXS*86 (Sheldrick, 1985)	*SHELXS*86 (Sheldrick, 1985)
Structure refinement	*SHELX*76 (Sheldrick, 1976)	*SHELX*76 (Sheldrick, 1976)	*SHELX*76 (Sheldrick, 1976)	*SHELX*76 (Sheldrick, 1976)	*SHELX*76 (Sheldrick, 1976)
Preparation of material for publication	*PLATON*93 (Spek, 1993)	*PLATON*93 (Spek, 1993)	*PLATON*93 (Spek, 1993)	*PLATON*93 (Spek, 1993)	*PLATON*93 (Spek, 1993)

isomers) were optimized with PM3 (Stewart, 1989*a*,*b*; Dewar *et al.*, 1990; Stewart, 1990*c*) in *MOPAC* 6.0 (Stewart, 1990*a*,*b*). The EF minimizer and the PRECISE level of precision were used, and the average polarizability, principal moments of inertia and other molecular properties were calculated. More than 20 electronic and geometric variables were studied with *Cricket Graph* 1.3 (1988) and only those having the correlation coefficient $R = 0.70$ with lipophilicity were used for further analyses. Selected variables were used for principal component analysis (PCA; Beebe & Kowalski, 1987; Sharaf *et al.*, 1986; Taylor & Allen, 1994) performed with *Matlab* 5.2 (1998). The data were autoscaled with unit variance. Principal component regressions (PCR; Beebe & Kowalski, 1987; Kowalski & Seasholtz, 1991) and multiple linear regression (MLR; Beebe & Kowalski, 1987) were performed using *Matlab* 5.2 (1998). In the analyses presented electronic structures of the substituents [C(H_3), Cl, F] are important; for this reason the van der Waals radii of the non-H atoms (C, Cl, F) were utilized rather than those of functional groups (CH_3). Also, the van der Waals radii of H atoms are experimental values and they vary among classes of compounds.

2.4. Physico-chemical measurements

The melting points stated above were determined in open capillaries and were not corrected. Molecular mass determinations were performed on an EXTREL Fourier transform mass spectrometer, using electron impact ionization at 70 eV. UV spectra were recorded on a Pye Unicam Philips PU 8700 computerized one-beam UV–vis spectrophotometer. ^{1}H NMR spectra (internal standard: tetramethylsilane) were obtained in acetone-d_6 solution, at sample concentrations of 75–95 mmol dm^{-3}, on a Varian Gemini 300 instrument operating at 300 MHz.

For lipophilicity studies, 20 × 20 cm glass plates coated with silica gel 60 GF 254 (Merck), to a thickness of 0.3 mm, were impregnated by developing with a 10% solution of *n*-octanol in acetone, dried briefly at 323 K, before sample application, and finally developed, at 277 K with McIlvain (0.1 *M* citrate/phosphate) buffer, pH 6.0, saturated with *n*-octanol. Indoles were visualized by spraying with 1% 4-dimethylaminobenzaldehyde in ethanol/concentrated HCl (1:1). The increment in lipophilicity caused by substitution at the indole nucleus (Leo *et al.*, 1971) was then computed as $\Pi = \log P^{\text{substituted IAA}} - \log P^{\text{IAA}} = R_M^{\text{substituted IAA}} - R_M^{\text{IAA}}$. In these expressions P represents the partition coefficient between an organic phase, such as *n*-octanol or the C_{18} stationary phase used in HPLC, and an aqueous phase, *i.e.* for the data discussed here, a buffer (TLC, 'shake-flask method') or 0.1 *N* acetic acid in 25% aqueous acetonitrile (HPLC). R_M was computed from the chromatographic mobility, R_F, as $\log(1/R_F - 1)$. If determined by TLC, Π was calculated from R_M values determined on the same plate. The values listed in Table 9 were averaged from up to 15 individual chromatograms.

2.5. Bioassays

The auxin activity of indole-3-acetic acid and its ring-alkylated analogues was compared in an oat (*Avena*) coleoptile straight-growth test, as described by Larsen (1961) and Mitchell & Livingston (1968). Seeds of *Avena sativa* L. cv. Pula were soaked in tap water for 6 h, sown onto moist vermiculite and germinated at 300 K for 4 d in complete darkness, except for short daily exposure to red light. Coleoptiles, 20–30 mm in

Table 2
Experimental details.

	6-Et-IAA
Crystal data	
Chemical formula	$C_{12}H_{13}NO_2$
Chemical formula weight	203.24
Cell setting	Monoclinic
Space group	$P2_1/c$
a (Å)	22.455 (1)
b (Å)	5.286 (1)
c (Å)	9.313 (1)
β (°)	110.89 (1)
V (Å^3)	1032.76 (10)
Z	4
D_x (Mg m^{-3})	1.307
Radiation type	Mo $K\alpha$
Wavelength (Å)	0.71073
No. of reflections for cell parameters	25
θ range (°)	5–13
μ (mm^{-1})	0.0964
Temperature (K)	103
Crystal form	Plate
Crystal size (mm)	0.30 × 0.20 × 0.06
Crystal colour	Colourless
Data collection	
Diffractometer	Enraf–Nonius CAD-4
Data collection method	$\omega/2\theta$ scans
Absorption correction	None
No. of measured reflections	2917
No. of independent reflections	1476
No. of observed reflections	814
Criterion for observed reflections	$I > 2\sigma(I)$
R_{int}	0.052
θ_{max} (°)	25
Range of h, k, l	$-23 \rightarrow h \rightarrow 24$ $0 \rightarrow k \rightarrow 6$ $-7 \rightarrow l \rightarrow 10$
No. of standard reflections	3
Frequency of standard reflections	Every 87 reflections
Intensity decay (%)	2.4
Refinement	
Refinement on	F
R	0.062
wR	0.052
S	0.91
No. of reflections used in refinement	814
No. of parameters used	153
H-atom treatment	H atoms riding
Weighting scheme	$w = 3.591/[\sigma^2(F_o) + 0.000091(F_o^2)]$
$(\Delta/\sigma)_{max}$	0.05
$\Delta\rho_{max}$ (e Å^{-3})	0.23
$\Delta\rho_{min}$ (e Å^{-3})	−0.28
Extinction method	None
Source of atomic scattering factors	*International Tables for Crystallography* (1992, Vol. C, Tables 4.2.6.8 and 6.1.1.4)
Computer programs	
Data collection	*CAD*-4 (Enraf–Nonius, 1988)
Cell refinement	*CAD*-4 (Enraf–Nonius, 1988), *CELDIM* routine
Data reduction	*SDP* (B. A. Frenz & Associates Inc., 1982)
Structure solution	*SHELXS*86 (Sheldrick, 1985)
Structure refinement	*SHELX*76 (Sheldrick, 1976)
Preparation of material for publication	*PLATON*93 (Spek, 1993)

Table 3
Fractional atomic coordinates and equivalent isotropic displacement parameters (Å^2) for 2-Me-IAA.

$$U_{eq} = (1/3)\Sigma_i\Sigma_j U^{ij} a^i a^j \mathbf{a}_i.\mathbf{a}_j.$$

	x	y	z	U_{eq}
O1	0.9544 (2)	−0.0794 (1)	0.8285 (2)	0.0583 (6)
O2	0.8698 (2)	0.0681 (1)	0.8907 (2)	0.0692 (7)
N1	0.5467 (3)	0.2278 (2)	0.5059 (2)	0.0568 (7)
C2	0.6732 (3)	0.1639 (2)	0.5051 (2)	0.0502 (8)
C3	0.6586 (3)	0.0868 (2)	0.6046 (2)	0.0468 (7)
C4	0.4384 (4)	0.0496 (2)	0.7716 (3)	0.0617 (10)
C5	0.2965 (4)	0.0862 (3)	0.8023 (4)	0.0774 (13)
C6	0.2313 (4)	0.1739 (3)	0.7354 (4)	0.0779 (13)
C7	0.3063 (3)	0.2276 (2)	0.6360 (3)	0.0667 (10)
C8	0.7676 (4)	0.0000 (2)	0.6379 (3)	0.0569 (9)
C9	0.8678 (3)	0.0001 (2)	0.7971 (3)	0.0446 (7)
C10	0.7939 (4)	0.1848 (2)	0.4057 (4)	0.0760 (11)
C31	0.5171 (3)	0.1024 (2)	0.6679 (2)	0.0483 (7)
C71	0.4486 (3)	0.1914 (2)	0.6023 (2)	0.0504 (8)

Table 4
Fractional atomic coordinates and equivalent isotropic displacement parameters (Å^2) for 4-Me-IAA.

$$U_{eq} = (1/3)\Sigma_i\Sigma_j U^{ij} a^i a^j \mathbf{a}_i.\mathbf{a}_j.$$

	x	y	z	U_{eq}
O1	0.5521 (1)	0.2131 (1)	1.0514 (1)	0.0212 (3)
O2	0.5873 (1)	0.0922 (1)	0.9217 (1)	0.0189 (3)
N1	0.8154 (1)	0.4957 (2)	0.7507 (1)	0.0235 (4)
C2	0.6982 (2)	0.4966 (2)	0.7990 (1)	0.0241 (5)
C3	0.7464 (2)	0.4108 (2)	0.8795 (1)	0.0201 (4)
C4	1.0201 (2)	0.2654 (2)	0.9475 (1)	0.0233 (4)
C5	1.1639 (2)	0.2323 (2)	0.9242 (1)	0.0292 (5)
C6	1.1989 (2)	0.2872 (2)	0.8416 (1)	0.0286 (5)
C7	1.0911 (2)	0.3783 (2)	0.7789 (1)	0.0228 (4)
C8	0.6513 (2)	0.3986 (2)	0.9518 (1)	0.0257 (5)
C9	0.5967 (2)	0.2191 (2)	0.9725 (1)	0.0170 (4)
C10	0.9912 (2)	0.2127 (2)	1.0392 (1)	0.0310 (5)
C31	0.9056 (2)	0.3534 (2)	0.8825 (1)	0.0180 (4)
C71	0.9440 (2)	0.4098 (2)	0.8000 (1)	0.0187 (4)

length, were harvested under green light and 10 mm sections were excized starting 1–2 mm below the tip. They were temporarily stored (about 2 h) floating on distilled water and distributed, in aliquots of ten, to 3 cm polystyrene petri dishes containing 2.7 ml of auxin solution in glass-distilled water. A water control and a complete series of IAA dilutions were included in each set of bioassays. After 20 h of growth in darkness, at 300 K, shadow graphs (original size) of the sections on photographic paper were prepared and measured to the nearest 0.5 mm. The function

$$y = d + [a/s(x + c)] \exp\{-[\ln(x + c) - b]^2/2s^2\},$$

where y is the length of coleoptile section in mm, x −log(auxin concentration in mol dm^{-3}), and a, b, c, d and s are shape parameters optimized by the fitting process, and fourth- and fifth-degree polynomials were fitted to the dose–response data; the curve optimally presenting the data points was used to estimate the maximal elongation and the optimal and half-optimal concentrations. The growth-promoting effects thus

Table 5
Fractional atomic coordinates and equivalent isotropic displacement parameters (Å^2) for 6-Me-IAA.

$U_{eq} = (1/3)\Sigma_i\Sigma_j U^{ij} a^i a^j \mathbf{a}_i.\mathbf{a}_j$.

	x	*y*	*z*	U_{eq}
O1	0.0216 (5)	0.5280 (1)	1.1766 (3)	0.0625 (11)
O2	0.1625 (4)	0.5298 (1)	0.9238 (3)	0.0650 (11)
N1	0.7320 (6)	0.5899 (1)	0.8783 (4)	0.0530 (14)
C2	0.5665 (6)	0.5693 (1)	0.9324 (4)	0.0423 (12)
C3	0.4239 (5)	0.5887 (1)	1.0198 (4)	0.0366 (11)
C4	0.4350 (7)	0.6546 (1)	1.0885 (5)	0.0510 (16)
C5	0.5540 (7)	0.6840 (1)	1.0622 (5)	0.0607 (17)
C6	0.7456 (7)	0.6836 (1)	0.9691 (5)	0.0623 (17)
C7	0.8196 (7)	0.6530 (1)	0.9022 (5)	0.0560 (16)
C8	0.2243 (5)	0.5776 (1)	1.1089 (4)	0.0423 (12)
C9	0.1367 (6)	0.5429 (1)	1.0610 (5)	0.0453 (12)
C10	0.8722 (8)	0.7168 (1)	0.9436 (6)	0.094 (2)
C31	0.5057 (5)	0.6232 (1)	1.0204 (4)	0.0394 (11)
C71	0.6987 (5)	0.6234 (1)	0.9290 (4)	0.0426 (14)

Table 6
Fractional atomic coordinates and equivalent isotropic displacement parameters (Å^2) for 7-Me-IAA.

$U_{eq} = (1/3)\Sigma_i\Sigma_j U^{ij} a^i a^j \mathbf{a}_i.\mathbf{a}_j$.

	x	*y*	*z*	U_{eq}
O1	0.0107 (1)	0.7574 (4)	0.3874 (2)	0.0811 (6)
O2	0.0766 (1)	0.4041 (4)	0.4752 (2)	0.0743 (6)
N1	0.2671 (1)	0.2538 (4)	0.3218 (2)	0.0542 (6)
C2	0.1960 (1)	0.3372 (5)	0.2674 (3)	0.0565 (7)
C3	0.1828 (1)	0.5300 (5)	0.3466 (3)	0.0508 (6)
C4	0.2704 (1)	0.7386 (5)	0.5714 (3)	0.0616 (7)
C5	0.3411 (1)	0.7287 (6)	0.6591 (3)	0.0680 (7)
C6	0.3916 (1)	0.5545 (5)	0.6355 (3)	0.0637 (7)
C7	0.3736 (1)	0.3841 (5)	0.5252 (2)	0.0500 (6)
C8	0.1134 (1)	0.6829 (5)	0.3196 (3)	0.0629 (7)
C9	0.0662 (1)	0.5992 (5)	0.4035 (3)	0.0552 (7)
C10	0.4284 (2)	0.2032 (6)	0.4975 (3)	0.0720 (7)
C31	0.2490 (1)	0.5697 (5)	0.4581 (2)	0.0467 (6)
C71	0.3014 (1)	0.3938 (5)	0.4391 (2)	0.0452 (6)

Table 7
Fractional atomic coordinates and equivalent isotropic displacement parameters (Å^2) for 4-Et-IAA.

$U_{eq} = (1/3)\Sigma_i\Sigma_j U^{ij} a^i a^j \mathbf{a}_i.\mathbf{a}_j$.

	x	*y*	*z*	U_{eq}
O1	0.0901 (3)	0.9177 (4)	−0.0898 (1)	0.0447 (8)
O2	0.1554 (2)	0.9165 (3)	0.0643 (1)	0.0427 (8)
N1	0.5646 (3)	0.7035 (4)	0.2082 (2)	0.0370 (9)
C2	0.4349 (4)	0.7608 (5)	0.1510 (2)	0.0338 (10)
C3	0.4470 (3)	0.7643 (4)	0.0610 (2)	0.0272 (9)
C4	0.6774 (3)	0.6834 (4)	−0.0070 (2)	0.0298 (10)
C5	0.8228 (4)	0.6282 (5)	0.0230 (2)	0.0384 (11)
C6	0.8888 (4)	0.5939 (5)	0.1171 (2)	0.0440 (11)
C7	0.8109 (4)	0.6144 (5)	0.1843 (2)	0.0411 (11)
C8	0.3287 (3)	0.8145 (5)	−0.0238 (2)	0.0297 (10)
C9	0.1852 (3)	0.8867 (4)	−0.0098 (2)	0.0283 (9)
C10	0.6073 (4)	0.7177 (5)	−0.1083 (2)	0.0327 (10)
C11	0.7026 (5)	0.6843 (7)	−0.1775 (2)	0.0465 (14)
C31	0.5956 (3)	0.7070 (4)	0.0616 (2)	0.0277 (9)
C71	0.6651 (3)	0.6708 (4)	0.1556 (2)	0.031 (1)

found for IAA and its ring-alkylated derivatives in the *Avena* coleoptile straight-growth test are listed in Table 10.

Table 8
Fractional atomic coordinates and equivalent isotropic displacement parameters (Å^2) for 6-Et-IAA.

$U_{eq} = (1/3)\Sigma_i\Sigma_j U^{ij} a^i a^j \mathbf{a}_i.\mathbf{a}_j$.

	x	*y*	*z*	U_{eq}
O1	0.4866 (2)	0.2564 (7)	0.6155 (4)	0.0544 (18)
O2	0.43424 (18)	−0.1004 (7)	0.5175 (4)	0.0542 (14)
N1	0.2633 (3)	−0.2782 (8)	0.6324 (6)	0.059 (2)
C2	0.3246 (4)	−0.1955 (10)	0.7080 (7)	0.059 (3)
C3	0.3359 (4)	0.0156 (10)	0.6321 (7)	0.055 (3)
C4	0.2588 (4)	0.2437 (11)	0.3877 (7)	0.052 (3)
C5	0.1982 (4)	0.2344 (11)	0.2821 (7)	0.058 (3)
C6	0.1543 (4)	0.0466 (10)	0.2855 (8)	0.055 (3)
C7	0.1724 (4)	−0.1369 (10)	0.3998 (7)	0.053 (3)
C8	0.3964 (3)	0.1657 (10)	0.6779 (7)	0.058 (3)
C9	0.4407 (3)	0.0919 (11)	0.5944 (6)	0.053 (3)
C10	0.0879 (4)	0.0487 (10)	0.1664 (8)	0.070 (3)
C11	0.0465 (4)	0.2574 (11)	0.1914 (9)	0.087 (4)
C31	0.2787 (4)	0.0611 (9)	0.5051 (7)	0.049 (3)
C71	0.2337 (4)	−0.1267 (10)	0.5067 (8)	0.056 (3)

Table 9
Lipophilicities (Π) of ring-alkylated and -halogenated indole-3-acetic acids estimated by thin-layer (TLC) and high-pressure liquid (HPLC) chromatographies.

TLC determined for the *dissociated* acids using *n*-octanol-impregnated silica gel layers developed with McIlvain (citrate–phosphate) buffer, pH 6.0. HPLC previously determined for the *undissociated* acids using a C18 column eluted with 25% aqueous acetonitrile containing 0.1 *N* acetic acid (Antolić *et al.*, 1996). Π values are based on the partition between *n*-octanol and phosphate buffer, pH 7.0, using the 'shake-flask method', may be computed from data given by Katekar & Geissler (1982) for: 4-chloroindole-3-acetic acid, 0.64; 5-chloroindole-3-acetic acid, 0.71; 6-chloroindole-3-acetic acid, 0.90; 7-chloroindole-3-acetic acid, 0.51.

	Lipophilicity parameter Π	
Compound	by TLC	by HPLC
Indole-3-acetic acid	0.00	0.00
2-Methylindole-3-acetic acid	0.47	0.18
4-Methylindole-3-acetic acid	0.16	0.23
4-Ethylindole-3-acetic acid	0.55	n.d.†
4-Fluoroindole-3-acetic acid	0.17	0.12
4-Chloroindole-3-acetic acid	0.53	0.31
5-Methylindole-3-acetic acid	0.50	0.32
5-Ethylindole-3-acetic acid	1.00	n.d.†
5-*n*-Propylindole-3-acetic acid	1.54	n.d.†
5-*n*-Butylindole-3-acetic acid	1.94	n.d.†
5-Fluoroindole-3-acetic acid	0.17	0.17
5-Chloroindole-3-acetic acid	1.13	0.49
5-Bromoindole-3-acetic acid	1.29	n.d.†
6-Methylindole-3-acetic acid	0.38	0.33
6-Ethylindole-3-acetic acid	1.01	n.d.†
6-Fluoroindole-3-acetic acid	0.20	0.19
6-Chloroindole-3-acetic acid	1.16	0.50
7-Methylindole-3-acetic acid	0.43	0.30
7-Fluoroindole-3-acetic acid	0.21	0.18
7-Chloroindole-3-acetic acid	1.00	0.45

† n.d. = not determined.

3. Results

3.1. Molecular structures in the crystalline state

Interatomic distances, bond and selected torsion angles for methyl- and ethylindole-3-acetic acids are listed in Tables 11, 12 and 13. This work includes the structure determination of

Table 10
Growth-promoting effect of IAA and its ring-alkylated derivatives in the *Avena* coleoptile straight-growth test.

Arithmetic means ± standard error. While the geometric mean is generally preferred for averaging logarithms, its values were, for the data presented in this table and within the limits of precision adopted, identical to the corresponding arithmetic means. Elongation effected by the optimal concentration of the respective auxin divided by the elongation caused by the optimal concentration of IAA in the same batch of coleoptile sections. Elongation was computed as the length of the auxin-treated coleoptile sections *minus* the length of coleoptile section in no-auxin controls.

Compound	Number of assays	Negative logarithm of optimal concentration	Relative optimal elongation	Negative logarithm of half-optimal concentration (in mol dm^{-3})
Indole-3-acetic acid	15	4.1 ± 0.0	1†	5.5 ± 0.1
2-Methylindole-3-acetic acid	6	3.7 ± 0.1	0.86 ± 0.07‡	4.7 ± 0.1
4-Methylindole-3-acetic acid	5	4.3 ± 0.1	1.49 ± 0.15	5.6 ± 0.2
4-Ethylindole-3-acetic acid	5	4.3 ± 0.1	0.58 ± 0.08	5.3 ± 0.1
5-Methylindole-3-acetic acid	5	4.2 ± 0.1	1.17 ± 0.11‡	5.3 ± 0.2
5-Ethylindole-3-acetic acid	4	4.3 ± 0.1	1.00 ± 0.04‡	5.6 ± 0.1
5-*n*-Propylindole-3-acetic acid	6	4.4 ± 0.1	0.74 ± 0.09	5.5 ± 0.1
5-*n*-Butylindole-3-acetic acid	4	4.4 ± 0.1	0.63 ± 0.08	5.4 ± 0.1
6-Methylindole-3-acetic acid	5	4.2 ± 0.1	1.13 ± 0.08‡	5.4 ± 0.1
6-Ethylindole-3-acetic acid	3	4.3 ± 0.2	0.68 ± 0.06‡	5.5 ± 0.2
7-Methylindole-3-acetic acid	4	4.2 ± 0.2	1.17 ± 0.21‡	5.5 ± 0.1

† By definition. ‡ In Students' t-test not significantly ($p = 0.05$) different from 1. This must be taken with caution, however, as three out of ten of the original data sets failed to pass a test (based on the ratio of the data range and the standard deviation) for normal distribution. Using the non-parametric test of Sachs (1978), the relative optimal elongations for all ring-substituted auxins tested, except 5-ethylindole-3-acetic acid, were significantly ($p = 0.05$) different from 1.

Table 11
Bond lengths (Å) for alkylated indole-3-acetic acids.

Bond lengths for IAA to be published, see §3.1. For 5-Me-IAA and 5-Et-IAA values, see Kojić-Prodić *et al.* (1991).

	IAA	2-Me-IAA	4-Me-IAA	5-Me-IAA	6-Me-IAA	7-Me-IAA	4-Et-IAA	5-Et-IAA
N1—C2	1.366 (3)	1.380 (4)	1.366 (2)	1.365 (3)	1.371 (5)	1.373 (3)	1.368 (5)	1.373 (5)
N1—C71	1.380 (3)	1.367 (3)	1.373 (2)	1.371 (3)	1.372 (5)	1.370 (3)	1.369 (4)	1.376 (6)
C2—C3	1.367 (3)	1.363 (3)	1.364 (2)	1.355 (4)	1.356 (5)	1.349 (4)	1.361 (4)	1.365 (5)
C3—C31	1.434 (3)	1.424 (3)	1.441 (2)	1.431 (3)	1.426 (5)	1.428 (3)	1.443 (4)	1.424 (6)
C3—C8	1.492 (3)	1.488 (4)	1.497 (2)	1.488 (3)	1.495 (5)	1.497 (3)	1.508 (4)	1.502 (5)
C31—C4	1.404 (3)	1.399 (4)	1.412 (2)	1.397 (3)	1.401 (5)	1.395 (4)	1.413 (4)	1.395 (6)
C31—C71	1.413 (3)	1.406 (4)	1.417 (2)	1.405 (3)	1.406 (4)	1.411 (3)	1.414 (4)	1.411 (5)
C4—C5	1.381 (3)	1.374 (5)	1.387 (2)	1.381 (3)	1.372 (6)	1.373 (4)	1.382 (5)	1.368 (5)
C5—C6	1.404 (3)	1.385 (5)	1.402 (2)	1.396 (3)	1.406 (6)	1.396 (3)	1.405 (4)	1.410 (5)
C6—C7	1.378 (3)	1.361 (4)	1.373 (2)	1.362 (4)	1.377 (6)	1.377 (4)	1.367 (5)	1.356 (6)
C7—C71	1.388 (3)	1.385 (4)	1.398 (2)	1.384 (3)	1.385 (5)	1.390 (3)	1.386 (5)	1.382 (5)
C8—C9	1.506 (3)	1.492 (4)	1.502 (2)	1.498 (3)	1.497 (5)	1.507 (3)	1.496 (4)	1.492 (6)
C9—O1	1.314 (3)	1.300 (3)	1.323 (2)	1.307 (3)	1.306 (5)	1.308 (3)	1.320 (3)	1.301 (5)
C9—O2	1.224 (3)	1.217 (3)	1.225 (2)	1.209 (3)	1.223 (5)	1.211 (3)	1.211 (3)	1.214 (5)
C2—C10		1.475 (4)						
C4—C10			1.507 (2)				1.508 (4)	
C5—C10				1.506 (4)				1.508 (6)
C6—C10					1.518 (6)			
C7—C10						1.498 (4)		
C10—C11							1.521 (5)	1.505 (8)

six compounds. For comparison, 5-Me-IAA and 5-Et-IAA (Kojić-Prodić *et al.*, 1991) were included in Tables 11, 12 and 13, and also the native plant hormone 'indole-3-acetic acid' (auxin). The structure of the latter was determined by Karle *et al.* (1964) and by Chandrasekhar & Raghunathan (1982), but we include instead the results of our own as yet unpublished low-temperature study at 103 K (the cif file has been deposited – see footnote **1**). The molecular structures are shown in Figs. 1(*a*)–(*f*). Analysis of the molecular geometry of indole systems covers two aspects:

(i) the comparison of the experimental values for the free hormone and its derivatives to recognize the effect of substitution, and

(ii) the effect of conjugation in indole-3-acetic acid and characterization of indole as an aromatic system.

Analysis of the data presented (Tables 11 and 12) reveals that the indole aromatic system exhibits typical geometrical characteristics, in particular, the contraction of C4—C5 and C6—C7 bonds relative to C5—C6. The means and sample standard deviations for the eight structures in Table 11 are 1.377 (6) and 1.369 (9) Å, respectively. They are very similar to those for the 343 structures ($R < 0.06$) with an indole moiety found in the Cambridge Structural Database (Allen & Kennard, 1993; version 5.15, April 1998, actually used), where the means are 1.373 and 1.378 Å. The low-temperature data for IAA gave values of 1.381 (3) Å for C4—C5 and 1.378 (3) Å for C6—C7. *Ab initio* calculations performed for IAA in STO-3G (*GAMESS*; Tomić *et al.*, 1995) reproduced the shortening of these bonds (both to 1.37 Å). Also, closing of the C6—C7—C71 angle [mean

Table 12
Bond angles (°) for alkylated indole-3-acetic acids.

Bond angles for IAA to be published, see §3.1. For 5-Me-IAA and 5-Et-IAA values, see Kojić-Prodić *et al.* (1991).

	IAA	2-Me-IAA	4-Me-IAA	5-Me-IAA	6-Me-IAA	7-Me-IAA	4-Et-IAA	5-Et-IAA
C2—N1—C71	109.5 (2)	110.0 (2)	109.1 (1)	109.9 (2)	109.9 (3)	109.4 (2)	108.9 (3)	109.5 (3)
N1—C2—C3	110.1 (2)	108.2 (2)	110.1 (2)	110.3 (2)	109.5 (3)	109.8 (2)	110.3 (3)	109.2 (9)
C2—C3—C8	126.8 (2)	126.5 (2)	124.1 (2)	126.5 (2)	129.2 (4)	126.8 (2)	127.3 (3)	128.9 (4)
C2—C3—C31	106.3 (2)	107.7 (2)	106.9 (1)	106.4 (2)	106.6 (3)	106.8 (2)	106.6 (3)	107.2 (3)
C31—C3—C8	126.9 (2)	125.8 (2)	128.8 (1)	127.1 (2)	124.2 (3)	126.3 (2)	126.1 (3)	123.9 (4)
C3—C31—C4	134.1 (2)	134.6 (3)	134.4 (2)	134.3 (2)	134.3 (3)	134.5 (2)	135.0 (3)	134.5 (3)
C3—C31—C71	107.4 (2)	107.0 (2)	106.1 (1)	107.1 (2)	107.9 (3)	107.3 (2)	106.2 (2)	107.2 (3)
C4—C31—C71	118.5 (2)	118.4 (2)	119.5 (2)	118.5 (2)	117.8 (3)	118.2 (2)	118.9 (3)	118.3 (4)
C31—C4—C5	119.1 (2)	118.5 (3)	116.9 (1)	119.9 (2)	119.2 (4)	119.1 (2)	117.1 (3)	120.7 (4)
C4—C5—C6	121.0 (2)	121.9 (3)	122.7 (2)	119.4 (2)	122.0 (4)	120.9 (3)	122.6 (3)	118.9 (4)
C5—C6—C7	121.4 (2)	120.9 (3)	121.2 (2)	122.4 (2)	120.0 (4)	122.5 (2)	121.1 (3)	122.4 (4)
C6—C7—C71	117.5 (2)	118.1 (3)	117.1 (1)	117.8 (2)	117.8 (4)	115.7 (2)	117.2 (3)	118.0 (4)
C31—C71—C7	122.6 (2)	122.2 (2)	122.5 (2)	121.9 (2)	123.3 (4)	123.6 (2)	123.2 (3)	121.7 (3)
N1—C71—C7	130.7 (2)	130.8 (2)	129.7 (1)	130.9 (2)	130.6 (3)	129.8 (2)	128.8 (3)	131.5 (3)
N1—C71—C31	106.7 (2)	107.0 (2)	107.9 (1)	107.2 (2)	106.2 (3)	106.6 (2)	108.0 (3)	106.8 (3)
C3—C8—C9	115.0 (2)	114.9 (2)	116.9 (1)	113.7 (2)	115.8 (3)	115.0 (2)	118.3 (2)	116.3 (3)
C8—C9—O1	113.2 (2)	114.2 (2)	112.4 (1)	113.4 (2)	114.3 (3)	112.4 (2)	111.7 (3)	114.1 (3)
C8—C9—O2	123.8 (2)	123.7 (2)	125.0 (1)	124.5 (2)	123.7 (4)	124.5 (2)	126.2 (3)	123.6 (3)
O1—C9—O2	123.0 (2)	122.1 (2)	122.6 (1)	122.1 (2)	122.0 (4)	123.1 (2)	122.1 (3)	122.4 (4)
N1—C2—C10		120.6 (2)						
C3—C2—C10		131.1 (2)						
C31—C4—C10			122.3 (2)				120.8 (3)	
C5—C4—C10			120.7 (1)				122.1 (3)	
C4—C10—C11							117.1 (3)	
C4—C5—C10				120.7 (2)				121.1 (3)
C6—C5—C10				119.9 (2)				120.0 (3)
C5—C6—C10					120.1 (4)			
C7—C6—C10					119.9 (4)			
C5—C10—C11								112.7 (4)
C6—C7—C10						122.4 (2)		
C71—C7—C10						121.9 (2)		

Table 13
Selected torsion angles (°) for alkylated indole-3-acetic acids.

Torsion angles for IAA to be published, see §3.1. For 5-Me-IAA and 5-Et-IAA values, see Kojić-Prodić *et al.* (1991).

	IAA	2-Me-IAA	4-Me-IAA	5-Me-IAA	6-Me-IAA	7-Me-IAA	4-Et-IAA	5-Et-IAA	6-Et-IAA
C2—C3—C8—C9	−96.9 (3)	108.5 (3)	115.3 (2)	91.1 (3)	17.7 (5)	102.5 (3)	6.7 (5)	−19.3 (6)	96.4 (8)
C31—C3—C8—C9	84.4 (3)	−73.6 (3)	−71.1 (2)	−85.0 (3)	−166.0 (3)	−80.8 (3)	−174.6 (3)	163.2 (3)	−84.5 (8)
C3—C8—C9—O1	−169.4 (2)	175.5 (2)	163.0 (1)	173.9 (2)	−154.8 (3)	172.8 (2)	−177.3 (3)	156.3 (3)	167.9 (5)
C3—C8—C9—O2	11.5 (3)	−4.5 (4)	−19.9 (2)	−7.4 (4)	27.8 (5)	−9.2 (4)	3.2 (5)	−26.5 (6)	−12.7 (8)
C31—C4—C10—C11							−178.5 (3)		
C5—C4—C10—C11							−1.5 (5)		
C4—C5—C10—C11								−92.5 (5)	
C6—C5—C10—C11								84.6 (5)	
C5—C6—C10—C11									−73.2 (9)
C7—C6—C10—C11									106.0 (7)

117.5 (3)° for seven structures in Table 12] and opening of the C31—C71—C7 angle [mean 122.7 (3)°] were detected in the phenyl part of the indole moiety. The geometry of unsubstituted indole-3-acetic acid revealed the same effects (for room-temperature data see Chandrasekhar & Raghunathan, 1982). Comparison of the bond lengths observed in alkylated indole-3-acetic acids (this work and Kojić-Prodić *et al.*, 1991) with those in unsubstituted indole-3-acetic acid revealed differences of ∼4 standard deviations. Thus, the effect of substitution on bond lengths is in most cases small and of the same order of magnitude as the experimental errors.

In the structures of alkylated IAAs there are a few examples of bond angles which significantly deviate from the hybridization type: the contraction of the angles at the substitution site 4 [C31—C4—C5, 116.9 (1)° for 4-Me-IAA and 117.1 (3)° for 4-Et-IAA] is accompanied by opening of the angle C4—C5—C6 [122.7 (2)° for 4-Me-IAA and 122.6 (3)° for 4-Et-IAA] in order to compensate deviations from a hexagon with an optimally conjugated electronic system. However, in the series of halogenated IAAs the angles at all the sites of the substitutions are in the ranges 122.3 (4)–124.8 (6)° for fluorinated derivatives and 121.7 (3)–122.7 (3)° for the chlorinated analogues.

In order to study the effect of conjugation in indole-3-acetic acid, indole and indene semi-empirical calculations (*MOPAC* 6.0, PM3) were carried out to generate geometrical parameters. Their comparison revealed a significant contribution from conjugation effects, particularly on the bond C3—C31 in indole (1.441 Å) and indole-3-acetic acid (1.443 Å), whereas in indene (1.500 Å) this effect is significantly smaller. Very good agreement of the values for indole and indole-3-acetic acid are supported by the experimental evidence from FT-IR spectroscopic studies (Lutz *et al.*, 1996). These data revealed that the $\nu_{C=O}$ vibrations are not affected by substitutions, which indicates that the $-CH_2$ group acts as a relatively efficient insulator between the conjugated π-systems of indole and the carboxylic acid group. Thus, the π-system of indole is electronically mostly independent. The mean value for the experimental bond lengths in the indole ring in IAA is

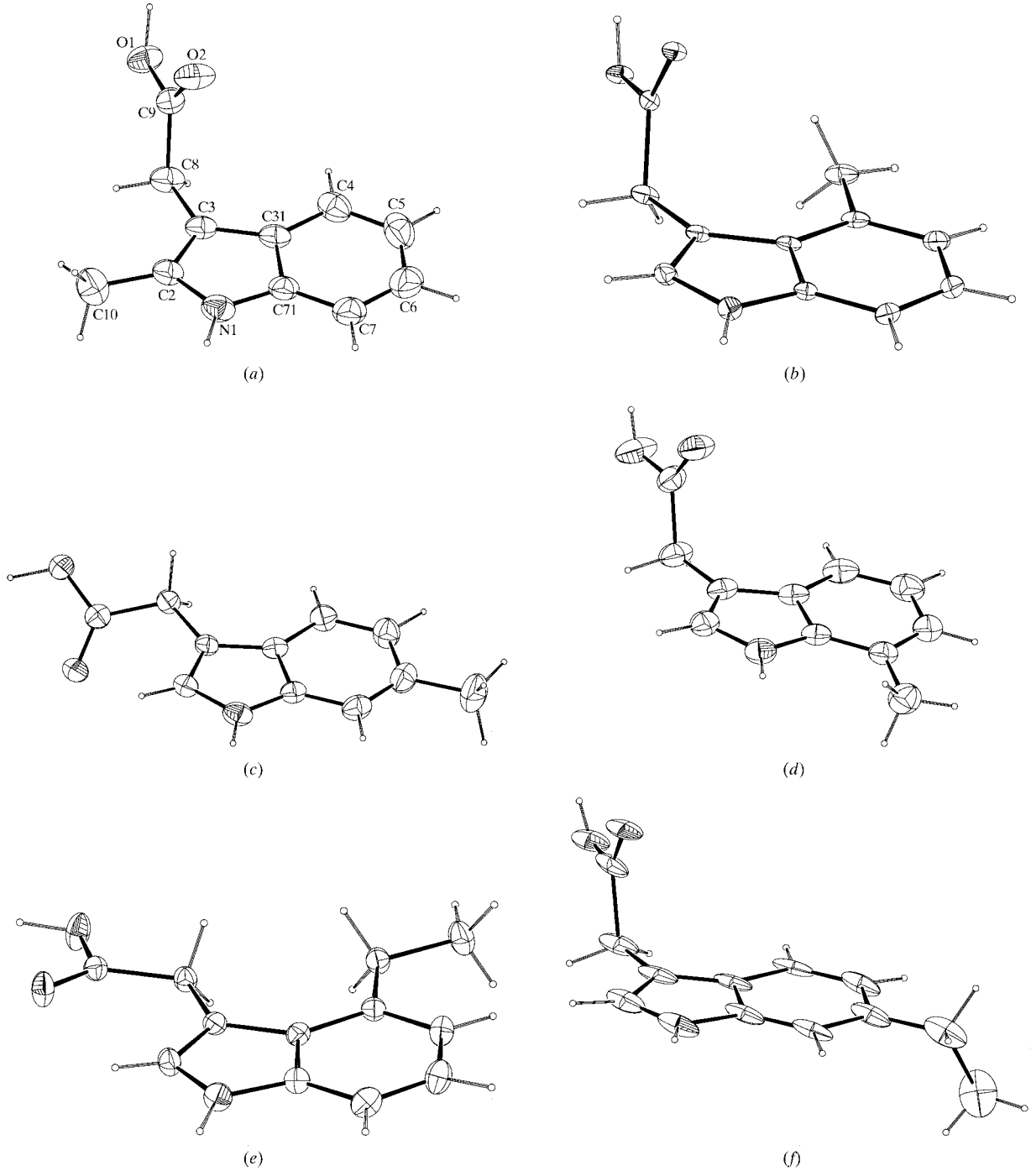

Figure 1
Molecular structures (*ORTEP*II; Johnson, 1976) of alkylated indole-3-acetic acids: (*a*) 2-Me-IAA, (*b*) 4-Me-IAA, (*c*) 6-Me-IAA, (*d*) 7-Me-IAA, (*e*) 4-Et-IAA and (*f*) 6-Et-IAA. Atom numbering is shown for 2-Me-IAA. The thermal ellipsoids are scaled at the 30% probability level.

Table 14
Hydrogen bonds, C—H···O and N—H···C (phenyl) contacts in the structures of alkylated indole-3-acetic acids.

Compound		D—H···A (Å)	D—H (Å)	H···A (Å)	D—H···A (°)	Space group
2-Me-IAA	O1—H···O2^{i}	2.633 (2)	1.01 (3)	1.63 (3)	176 (3)	$P2_1/c$
	N1—H···C4^{ii}	3.637 (4)	0.90 (3)	2.74 (3)	171	
	N1—H···C5^{ii}	3.552 (4)	0.90 (3)	2.79 (3)	143	
4-Me-IAA	O1—H···O2^{iii}	2.692 (1)	0.98 (2)	1.71 (2)	176 (2)	$P2_1/n$
	N1—H···O2^{iv}	2.980 (2)	1.01 (2)	2.08 (2)	148 (2)	
6-Me-IAA	O1—H···O2^{v}	2.635 (5)	1.10 (5)	1.54 (5)	175 (4)	*Pbca*
	N1—H···C2^{vi}	3.344 (5)	0.75 (3)	2.60 (3)	173	
7-Me-IAA	O1—H···O2^{vii}	2.659 (3)	0.98 (2)	1.69 (2)	168 (1)	$P2_1/c$
	N1—H···C5^{ii}	3.521 (3)	0.88 (1)	2.65 (1)	172	
4-Et-IAA	O1—H···O2 ^{viii}	2.695 (3)	0.96 (5)	1.74 (5)	174 (4)	$P2_1/n$
	N1—H···O1^{ix}	3.074 (3)	0.91 (4)	2.17 (4)	172 (3)	
6-Et-IAA	O1—H···O2^{x}	2.635 (6)	1.03 (7)	1.61 (7)	170 (6)	$P2_1/c$
	C2—H···O2^{xi}	3.236 (8)	1.08 (1)	2.16 (1)	172 (1)	
	N1—H···C5^{xi}	3.369 (9)	1.009 (8)	2.37 (1)	169 (1)	

Symmetry codes: (i) $-x+2, -y, -z+2$; (ii) $x, -y+\frac{1}{2}, z-\frac{1}{2}$; (iii) $-x+1, -y, -z+2$; (iv) $-x+\frac{3}{2}, y+\frac{1}{2}, -z+\frac{3}{2}$; (v) $-x, -y+1, -z+2$; (vi) $x+\frac{1}{2}, y, -z+\frac{3}{2}$; (vii) $-x, -y+1, -z+1$; (viii) $-x, 2-y, -z$; (ix) $x+\frac{1}{2}, -y+\frac{3}{2}, z+\frac{1}{2}$; (x) $-x+1, -y, -z+1$; (xi) $x, -y-\frac{1}{2}, z+\frac{1}{2}$.

Table 15
UV absorption maxima for IAA and its alkylated derivatives in ethanol (95%) solution.

ε is expressed in mol dm^{-3}

Compound	$\lambda\lambda_{max}$ in mm (log ε)			
IAA	220.0 (4.528)	274.5 (3.765)†	280.5 (3.788)	290.0 (3.708)
2-Me-IAA	223.0 (4.459)	275.5 (3.762)†	281.0 (3.778)	289.5 (3.702)
4-Me-IAA‡	222.5 (4.540)	274.5 (3.821)	280.0 (3.813)	292.0 (3.677)
5-Me-IAA‡§	223.0 (4.463)	277.5 (3.740)	286.0 (3.728)	297.0 (3.578)
6-Me-IAA‡§	222.5 (4.550)	276.5 (3.719)	282.0 (3.729)	292.5 (3.643)
7-Me-IAA	220.0 (4.568)	273.0 (3.729)	279.5 (3.793)	290.0 (3.688)

† Shoulder ‡ For the set of compounds studied here, changes in the UV spectrum owing to extension of the alkyl chain were within the limits of experimental error. § Additional shoulders at 289.0 (log ε = 3.707; 5-Me-IAA) and 286.5 nm (log ε = 3.698; 6-Me-IAA).

1.386 (5) Å, which is similar to C—C in benzene, 1.394 (7) Å. These data suggest that the indole ring with its high degree of aromaticity is an electronically well balanced system with defined properties; for example, as a π-excessive molecule it forms π-complexes with acceptors such as 1,3,5-trinitrobenzene (Brown *et al.*, 1979).

The overall conformation of the molecules (Fig. 2) is described by two torsion angles: C2—C3—C8—C9 defines the relative orientation of a side chain with respect to the indole plane and C3—C8—C9—O2 describes the orientation of the carboxyl group (Table 13). In the series of alkylated IAAs two distinct orientations of the side chain are observed: synperiplanar and anticlinal (Klyne & Prelog, 1960). The folded conformation with the side chain almost perpendicular to the indole ring (anticlinal conformation) is detected in all chlorinated and fluorinated IAAs, and in the free hormone as well (Chandrasekhar & Raghunathan, 1982). However, for the ten ring-alkylated derivatives studied so far, including 5-Pr^{n}-IAA and 5-Bu^{n}-IAA (Kojić-Prodić *et al.*, 1991), both conformations occur with equal frequency (Fig. 2). This can be explained by the very small energy difference between these two conformations, as revealed by computational chemistry methods (Ramek *et al.*, 1995, 1996; Antolić *et al.*, 1996; Nigović *et al.*, 1996). The conformation about the C8—C9 bond is (±)synperiplanar (Table 13).

3.2. Crystal packing

Among the six crystal structures the crystal packings of 6-Me-IAA and 4-Me-IAA were selected for illustration (Figs. 3 and 4). In the crystal structures presented there are two chemically distinct hydrogen bonds connecting:

(i) carboxyl groups, O1—H···O2, and

(ii) indole and carboxyl groups, N1—H···O1 (Table 14).

They form essentially two different patterns, the first with O—H···O dimers closing an eight-membered ring [$R_2^2(8)$; Etter *et al.*, 1990; Bernstein *et al.*, 1995] and the second with both types of hydrogen bonds O—H···O and N—H···O. The crystal structures of 2-Me-IAA, 6-Me-IAA (Fig. 3), 7-Me-IAA and 6-Et-IAA are characterized by hydrogen-bonded dimers, the pattern detected in the free hormone (Chandrasekhar & Raghunathan, 1982) and many organic carboxylic acids. The structures of 4-Me-IAA (Fig. 4) and 4-Et-IAA, in addition to hydrogen-bonded dimers, include the formation of an infinite chain $C(6)$ *via* N1—H···O. In the structure of 4-Me-IAA a carbonyl oxygen (O2) functions as the acceptor, whereas in the structure of 6-Me-IAA a hydroxyl oxygen (O1) participates in that hydrogen bond. In addition to the classical type of hydrogen bonds detected in the structures studied, weak C—H···O interactions between C sp^2 and C=O of the carboxyl group [Taylor & Kennard, 1982; 4.19–8.37 kJ mol^{-1} (Desiraju, 1991; Viswamitra *et al.*, 1993)] were observed. An intermolecular C2—H···O2 (in 6-Et-IAA) with a C···O distance of 3.236 (8), H···O 2.16 (1) Å and a C—H···O angle of 172 (1)° satisfied the criteria given for hydrogen bonds of this type (Nigović *et al.*, 1996, and references therein). The crystal structures lacking the hydrogen bonds of the N—H···O type revealed N—H···C(phenyl) interactions (Table 14), as was also observed in the series of halogenated IAAs (Nigović *et al.*, 1996; Antolić *et al.*, 1996). The geometrical criteria specified by Perutz (1993), Levitt & Perutz (1988) and Starikov & Steiner (1998) for this type of hydrogen bond can be applied to those detected in the series of alkylated IAAs (Table 14).

3.3. Spectroscopy

The influence of ring-alkylation on the electron distribution in the indole nucleus was checked by UV and ^{1}H NMR spectroscopies. The positions of the UV absorbance maxima (Table 15) were closer to those of unsubstituted IAA than in the case of ring-fluorinated and -chlorinated derivatives (Antolić *et al.*, 1996), all of which are active auxins. Alkylation at ring positions 2, 4, 5, 6 and 7 should thus not significantly disturb molecular orbital energy levels in terms of affinities to the postulated (Katekar, 1979) π-complexing sites of auxin-binding proteins. Changes in electron densities at individual ring positions, which may affect more specific recognition patterns, were estimated from ^{1}H NMR spectra (Table 16). The electron-releasing properties of an alkyl substituent in any of the ring positions examined were clearly reflected by a general upfield shift [$\Delta_{NMR} = \delta$ (alkyl-IAA) $- \delta$(IAA)] for all ring protons, although the effect was smaller than for many

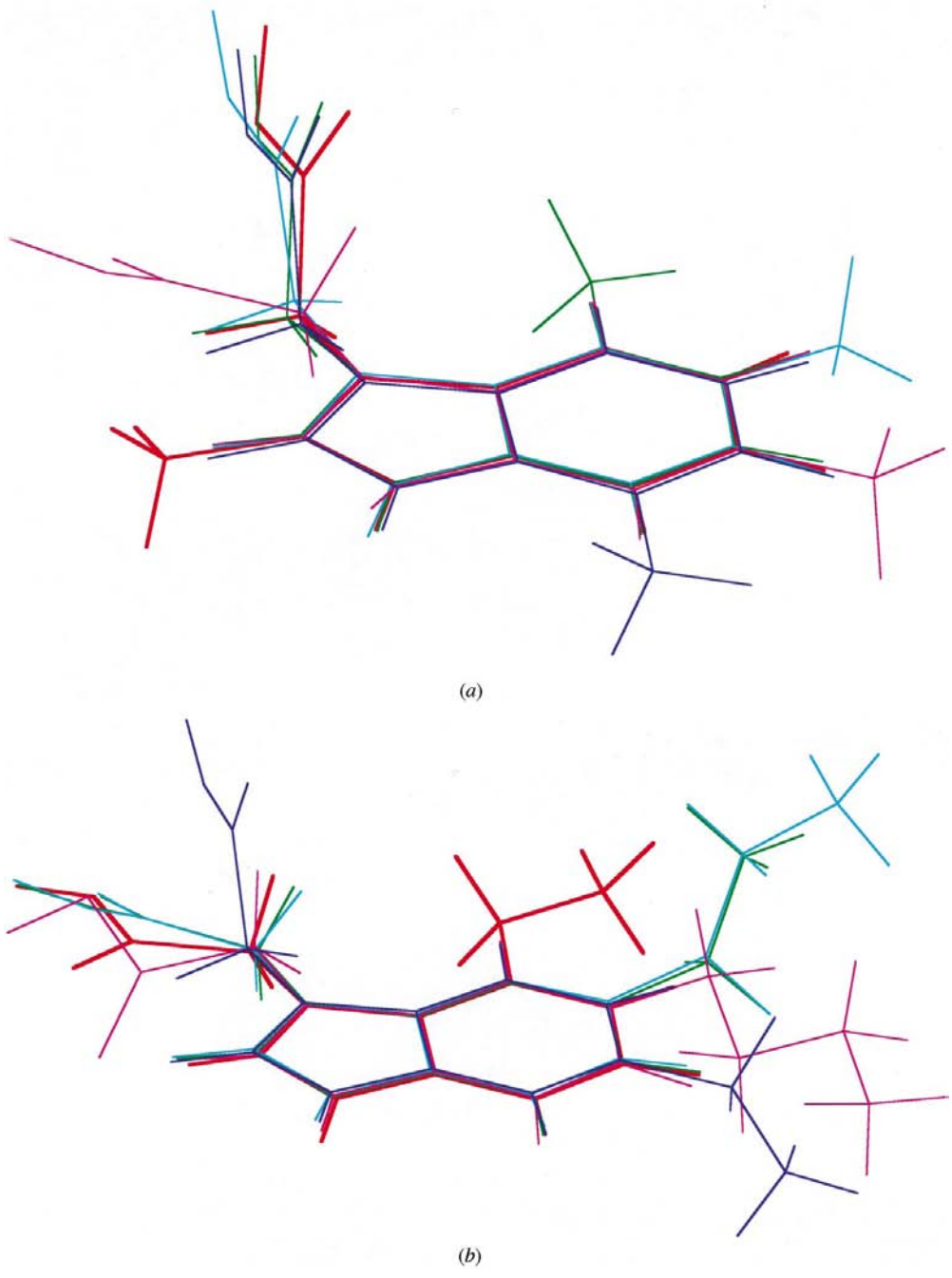

Figure 2
Overlap of observed conformations of alkylated IAAs (Kojić-Prodić *et al.*, 1991, and this work): (*a*) 2-Me-IAA, red, 4-Me-IAA, green, 5-Me-IAA, light blue, 6-Me-IAA, pink, 7-Me-IAA, dark blue; (*b*) 4-Et-IAA, red, 5-Et-IAA, green, 5-Pr^n-IAA, light blue, 5-Bu^n-IAA, pink, and 6-Et-IAA, dark blue.

Table 16
^{1}H NMR data [300 MHz, $(CD_3)_2CO$] for IAA and its alkylated derivatives.

Compound	Chemical shift values (δ, p.p.m.)								
	H-1	H-2	H-4	H-5	H-6	H-7	3-CH_2	CH_2-CH_3	
IAA†	10.12	7.29	7.60	7.03	7.10	7.39	3.75	–	–
2-Me-IAA	9.90	–	7.49	6.97	7.01	7.26	3.67	–	2.40
4-Me-IAA	10.02	7.20	–	6.74	6.95	7.20	3.91	–	2.65
4-Et-IAA	10.04	7.21	–	6.80	7.00	7.22	3.89	3.02	1.27
5-Me-IAA†	9.99	7.23	7.38	–	6.94	7.27	3.71	–	2.40
5-Et-IAA†	10.00	7.25	7.41	–	6.98	7.29	3.73	2.71	1.24
5-Pr-IAA†	9.99	7.24	7.40	–	6.97	7.29	3.72	2.66‡	0.94
5-Bu-IAA†	9.99	7.25	7.40	–	6.97	7.29	3.72	2.68‡	0.93
6-Me-IAA	9.91	7.17	7.47	6.87	–	7.17	3.72	–	2.39
6-Et-IAA	9.90	7.20	7.50	6.91	–	7.20	3.72	2.70	1.23
7-Me-IAA	10.04	7.26	7.44	6.95	6.91	–	3.74	–	2.47

Approximate J (Hz); within indole nucleus: 1, 2 = 2; 4, 5 = 7–8; 4, 6 = 1–2; 4, 7 = 1; 5, 6 = 7; 5, 7 = 1; 6, 7 = 8; side chain – ring protons: 2, CH_2COOH = 0.6–0.9; within alkyl chain: H, H_{vic} = 7.5 Hz

† Measured at 400 MHz (Ilić *et al.*, 1991). ‡ The methylene group adjacent to the indole nucleus.

other ring substituents (Morales-Ríos *et al.*, 1989). Alkylation shifts (Δ) within the benzene moiety ranged from 0.06 to 0.29 p.p.m. upfield, with $|\Delta_{ortho}| > |\Delta_{para}| > |\Delta_{meta}|$. Quantitative comparisons of the corresponding shifts for the H2 signal may be misleading because it overlaps with the H7 resonance in most of the compounds investigated. The position of the NH (H1) signal is of particular interest as this group has been proposed to be specifically recognized by auxin receptor proteins (Thimann, 1977). Alkylation shifts in this case decreased in the following order: 2-Me-IAA $\simeq$ 6-alkyl-IAA > 5-alkyl-IAA > 4-alkyl-IAA $\simeq$ 7-Me-IAA. A 6-alkyl group, which is formally in a *meta* position with respect to NH, thus had a larger effect than 5-(*para*)-alkyl. This would not be possible in the case of monocyclic benzene derivatives. However, the benzene moiety of the indole nucleus significantly deviates from the shape of a regular hexagon (§3.1, Tables 11 and 12), a fact which reflects electronic asymmetry. Also, the substituent effects which influence the NMR chemical shift of the NH signal are, in part, transmitted through the pyrrole moiety of the indole nucleus. Similar reasoning, supported by computational methods, has been used to rationalize the effect of 6-substituents on the deprotonation constant at the indole NH (Muñoz *et al.*, 1992), which, like the ^{1}H NMR shift, depends on the electron density at the ring nitrogen. For the resonance of the 3-CH_2 group, the small shift (−0.01 to −0.04 p.p.m.) observed on ring-alkylation in positions 5, 6 and 7 may mostly be a measure of experimental error. The corresponding larger shifts, upfield (−0.08 p.p.m.) for 2-Me-IAA and downfield (+0.14 to 0.16 p.p.m.) for 4-Me-IAA and 4-Et-IAA, could reflect steric influences of the 2- and 4-alkyl groups on the orientation of the spatially close (*cf.* §3.1), magnetically anisotropic (solvated) carboxyl moiety. It would be tempting to invoke similar anisotropy effects to explain the chemical shift difference between the methyl(ene) resonances at C4 and other ring positions. This interpretation is, however, *not* supported by the ^{1}H NMR spectra of structurally related indole derivatives which lack a carbonyl group.

3.4. Lipophilicity

The lipophilicity parameters (Π) of the alkyl-substituted indole-3-acetic acids studied in this work are summarized in Table 9. For comparison, the respective values for analogues substituted with halogens at the same ring positions are included. Due to the pH (6.0) of the eluent used and the

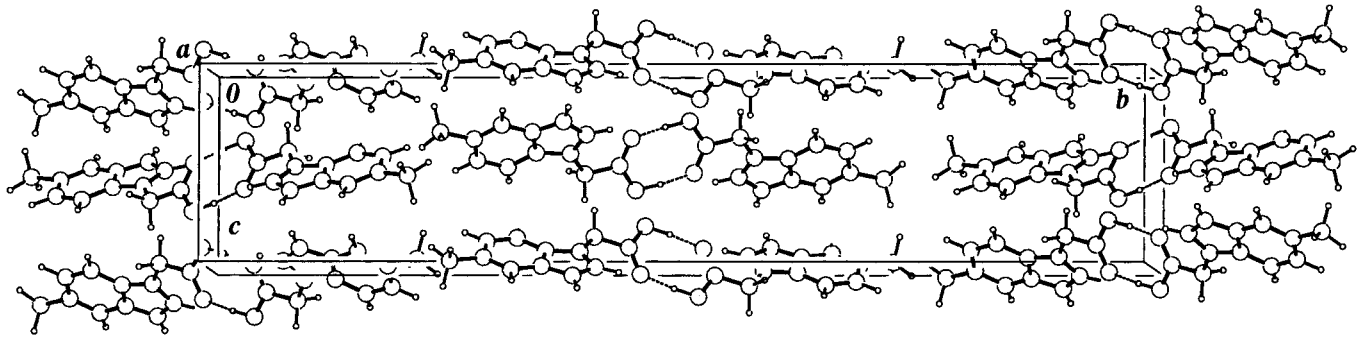

Figure 3
Molecular packing of 6-Me-IAA with hydrogen-bonded dimers around the inversion centre [$R_2^2(8)$].

Table 17
The data for average polarizability (E, in atomic units), principal moments of inertia around inertial axes Y and Z (I_2, I_3, in 10^{-40} g cm^2), relative molecular mass (M_r, in atomic units) and van der Waals radius (r_W, in Å) of the substituents.

Molecule	E	I_2	I_3	M_r	r_W
IAA†	94.327	1565.472	1942.715	1.079	1.0
4F-IAA	95.920	1656.005	2161.715	18.998	1.4
5F-IAA	96.081	1850.314	2427.276	18.998	1.4
6F-IAA	95.998	2152.384	2550.234	18.998	1.4
7F-IAA	95.889	2004.240	2408.537	18.998	1.4
2Me-IAA†	114.009	1527.359	2085.306	15.035	1.7‡
4Me-IAA	102.996	1615.753	2133.318	15.035	1.7‡
5Me-IAA	103.491	1812.006	2375.058	15.035	1.7‡
6Me-IAA	103.688	2095.271	2489.103	15.035	1.7‡
7Me-IAA	102.785	1951.011	2355.137	15.035	1.7‡
4Cl-IAA	103.726	1708.041	2447.900	35.453	1.8
5Cl-IAA	105.239	2205.073	2924.308	35.453	1.8
6Cl-IAA	105.830	2785.207	3188.821	35.453	1.8
7Cl-IAA	103.789	2458.912	2889.064	35.453	1.8

† Not used for PCA, PCR and MLR. ‡ The van der Waals radius of a C atom was used.

dissociation constants of IAA (pK = 4.6–4.7; Cohen *et al.*, 1958; Melhado *et al.*, 1981) and its ring-substituted derivatives (pK about the same as for IAA), the TLC method described above afforded lipophilicity data for the anions. The estimates

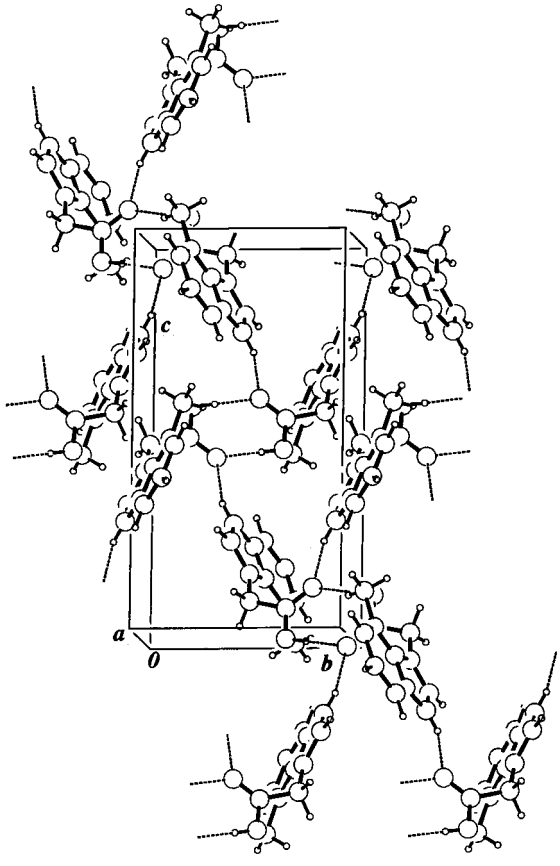

Figure 4
Molecular packing of 4-Me-IAA with O—H···O hydrogen bonds which connect molecules into dimers [$R_2^2(8)$]. N—H···O hydrogen bonds join molecules into an infinite chain (C6) along **c**.

Table 18
The correlation coefficient matrix for liphophilicity (Π) by HPLC, average polarizability (E), principal moments of inertia around inertial axes Y and Z (I_2, I_3), relative molecular mass (M_r) and van der Waals radius (r_W) of the substituents.

	Π	E	I_2	I_3	M_r	r_W
Π	1	0.867	0.730	0.844	0.704	0.859
E		1	0.374	0.496	0.466	0.985
I_2			1	0.933	0.569	0.352
I_3				1	0.777	0.492
M_r					1	0.550
r_W						1

for Π obtained in this way are close to the range of values previously found by partition between *n*-octanol and water in the classical 'shake-flask method' for a variety of aromatic systems (*e.g.* Kubinyi, 1993; Hansch *et al.*, 1963; Fujita *et al.*, 1964), including a selection of ring-chlorinated IAAs (Katekar & Geissler, 1982). For 13 out of the 20 compounds listed in Table 9, the lipophilicities of the *undissociated* forms were previously determined, in a different context, by reversed-phase HPLC on C_{18}-coated silica gel (Antolić *et al.*, 1996). The values obtained (Π_{HPLC}) are correlated to the TLC data by the regression: $\Pi_{TLC} = 2.67(\pm0.30) \times \Pi_{HPLC} - 0.28(\pm0.09)$ (s_{yx} = 0.31, r = 0.938). We interpret the highly significant correlation coefficient (r) to indicate that the dissociation of the carboxyl group is not accompanied by major changes in the solvatation of the remaining part of the auxin molecules. The value of the standard deviation with respect to regression ($s_{y.x}$) does, however, indicate minor group and position effects, which will be the subject of future research.

The fact that the lipophilicity of the anions and the undissociated molecules of ring-substituted IAAs are correlated facilitates the interpretation of structure–activity data. It is now assumed that auxin perception in plant cells preferentially takes place in the periplasmatic space. The growth response involves acidification of the periplasmic space, from pH 5.7 to 4.8–5.0 (Cleland, 1975). This affects the ratios of the dissociated and undissociated forms of ring-substituted IAAs, and thus their lipophilicities. The dissociated fractions of ring-substituted IAAs, and thus their lipophilicities, change accordingly. However, by virtue of the above correlation, these changes should occur in a commensurate fashion for the entire set of alkyl-IAAs studied here and the relative lipophilicities should remain about the same.

3.5. Plant growth-promoting activity

To our knowledge this is the first comprehensive experimental study covering the molecular structures and plant growth-promoting properties of IAA derivatives alkylated at ring positions 2–7. We have, however, previously reported on selected representatives of this group of compounds: the 5-alkyl-IAAs (alkyl = methyl, ethyl, *n*-propyl, *n*-butyl) and their biological activity in the *Avena* mesocotyl test (Kojić-Prodić *et al.*, 1991), and the ability of 4-Me-IAA and 4-Et-IAA to substitute for 4-Cl-IAA, the endogenous auxin which specifically regulates the growth of pea pericarps (Reinecke *et al.*,

Table 19
Eigenvalues for principal components together with percentage variance explained by each and the PRESS (PCR) values.

PC No.	Eigenvalue	% Variance	PRESS
1	6.12	68.11	0.0116
2	3.54	22.82	0.0095
3	2.16	8.48	0.0127
4	0.53	0.52	0.0121
5	0.19	0.07	0.0163

Table 20
The principal component loadings for average polarizability (E), principal moments of inertia around inertial axes Y and Z (I_2, I_3), relative molecular mass (M_r) and van der Waals radius (r_W) of the substituents.

	PC1	PC2	PC3	PC4	PC5
E	0.4338	−0.5421	0.2216	0.2488	0.6379
I_2	0.4263	0.4836	0.5003	0.5543	0.1636
I_3	0.4885	0.3858	0.0999	−0.7092	−0.3157
M_r	0.4436	0.1779	−0.8307	0.1908	0.2125
r_W	0.4413	−0.5401	0.0234	0.3024	0.6493

1999). Rescher *et al.* (1996) reported that *in vitro* binding affinities of 2-Me-, 4-Me-, 4-Et and 4-Cl-IAA to *Zea mays* auxin-binding protein (ABP1) correlated with their effects on the growth rate of corn coleoptiles. 4-Me-IAA was included in a study on auxin effects on stomatal aperture (Thomson *et al.*, 1988). The older literature only mentions 2-Me-IAA and 5-Me-IAA, which were prepared by Kögl & Kostermans as early as 1935 and were shown to be active in the *Avena* coleoptile curvature assay. The 5-isomer was considerably more effective than its 2-substituted analogue, but both were weaker auxins than IAA itself. Similar results were obtained in the *Avena* coleoptile straight-growth test (Muir *et al.*, 1949; Muir & Hansch, 1953) and the split pea-stem curvature assay (Hoffmann *et al.*, 1952; Porter & Thimann, 1965). In the tomato, 2-Me-IAA induced parthenocarpy (Sell *et al.*, 1952) if applied in sufficiently high concentrations and 5-Me-IAA was at least as effective as IAA in causing cell elongation and cell proliferation in stems and petioles (Hoffmann *et al.*, 1952).

In the *Avena* coleoptile straight-growth test, the auxins studied here gave dose–response curves of the form illustrated in Fig. 5. The shape parameters, averaged from a number of experiments, are presented in Table 10. The capacity to elongate depended on the batch of coleoptiles used. To compensate for this source of variability, the optimal elongation caused by ring-alkylated IAAs was divided by the optimal elongation effected by the unsubstituted parent compound in the same batch of coleoptiles. These ratios ('relative optimal elongation'; Table 10) proved to be fairly reproducible.

IAA and most of the ring-alkylated derivatives studied here started to exhibit growth-promoting activity at concentrations around 10^{-7} mol dm^{-3}. The dose–response curves then reached their half-optimal levels at $10^{-5.3}$–$10^{-5.6}$ (5.0–2.5×10^{-6}) mol dm^{-3}, peaked at $10^{-4.1}$–$10^{-4.4}$ (7.9–4.0×10^{-5}) mol dm^{-3}, and then steeply returned to control-level growth around 10^{-3} mol dm^{-3}. In fact, 5-Pr-IAA and 5-Bu-IAA appeared to be toxic at this concentration: the coleoptile sections lost turgor and elongated less than the water controls. Apart form these peculiarities at the top auxin concentrations examined, the dose–response curves were of the same general shape, and the small differences concerning optimal and half-optimal concentrations cannot be considered significant. The only auxin tested which did not follow this rule was 2-Me-IAA. Its dose–response curve covered an ∼100 times narrower range of concentrations, peaked at a 3–4 times higher concentration and reached its half-optimal level at a 6–8 times higher concentration.

What was most obviously different within the set of auxins studied was the optimal elongation relative to that caused by IAA. The influence of the alkyl group was the more pronounced the longer its carbon backbone and the closer the 3-CH_2COOH moiety. In the neighbouring 2-position, even a methyl group reduced elongation. 2-Et-IAA was reported to be without auxin activity (Kögl & Kostermans, 1935), but the compound was only tested in the *Avena* coleoptile curvature assay, which requires polar transport in addition to growth stimulating properties. In the 4-position, which is spatially close to the $-CH_2COOH$ moiety, a methyl group enhanced the elongation response, while the stimulatory effect in positions 5, 6 and 7 was less pronounced (*cf.* Table 10, second footnote‡). An ethyl group at C4 was, however, considerably more inhibitory than at C5, while its effect at C6 was intermediate. *n*-Propyl and *n*-butyl substituents, which could so far only be introduced at C5, reduced the optimal elongation to ∼60–75% of that achieved with IAA.

In a preliminary report (Antolić *et al.*, 1997), a somewhat different range of half-optimal concentrations (4.5–6.0×10^{-6} mol dm^{-3}) was given for the compounds studied here. Additional replicate experiments shifted this range to the set of values we now present in Table 10. The *Avena* mesocotyl test suggested differences in the half-optimal concentrations of IAA, 5-Me-IAA, 5-Et-IAA, 5-Pr-IAA and 5-Bu-IAA (Kojić-Prodić *et al.*, 1991), which were not seen in the coleoptile-section straight-growth test used here. While the mesocotyl test may be more sensitive to substituent effects, its main purpose in the work cited was to provide first *qualitative* proof for the growth-promoting activity of 5-Et-IAA, 5-Pr-IAA and 5-Bu-IAA; additional replicate experiments would be needed to provide firm *quantitative* data.

3.6. Quantitative structure–parameter relationship (QSPR)

Lipophilicity, a property important in biological effects, derived by a set of descriptors of additive nature, has been recognized as a useful parameter in QSAR (quantitative structure–activity relationships; Hansch & Fujita, 1964; Pliška *et al.*, 1996). A simple correlation between auxin activity and lipophilicity cannot be easily defined. Thus, the first step in the correlation search has been performed to connect lipophilicity with some physico-chemical parameters (QSPR) of the molecules of interest. Such a description starts with simple

Table 21
Results of the regression analyses.

The regression vector elements c_1–c_5 are coefficients of the equation $\Pi = c_1E + c_2I_2 + c_3I_3 + c_4M_r + c_5r_W$, where to the constant coefficient c_0 can be added if determined. The average deviation $\Delta = \Sigma|\Pi_{exp} - \Pi_{calc}|/12$. The correlation coefficient $r = [1 - \Sigma|\Pi_{exp} - \Pi_{calc}|^2/\Sigma|\langle\Pi_{exp}\rangle - \Pi_{calc}|^2]^{1/2}$. The standard error of prediction $sep = [\Sigma|\Pi_{exp} - \Pi_{calc}|^2/12]^{1/2}$. The F criterion $F = r^2(N - k - 1)/[k(1 - r^2)]$, $N = 12$, $k = 5$. The FIT criterion $FIT = F/(N + k^2)$.

Regression	c_1	c_2	c_3	c_4	c_5	Δ	r	sep	F	FIT	PRESS
MLR†	−0.0192	-1.13×10^{-4}	4.59×10^{-4}	-5.36×10^{-3}	0.8814	0.015	0.989	0.018	52.025	1.406	0.0174
MLR‡	6.13×10^{-4}	-6.93×10^{-5}	3.59×10^{-4}	-2.84×10^{-3}	0.4275	0.016	0.990	0.017	60.814	1.644	0.0258
PCR§	0.2900	0.1689	0.2128	0.2129	0.2937	0.019	0.977	0.026	25.102	0.678	0.0095

† MLR without the constant coefficient. ‡ MLR with the constant coefficient $c_0 = -1.1628$. § PCR based on the first two PCs. The regression vector is for autoscaled data.

geometrical and stereo-electronic parameters and extends to more sophisticated levels of intermolecular interactions. Lipophilicity is not only an empirical tool in structure–activity analysis, but also reveals the very complex dynamic interplay of intermolecular forces and intramolecular interactions. In this case, of particular interest is the interplay between positional isomerism (various substituents at different sites of the aromatic ring) and lipophilicity.

QSPR analysis uses some values obtained from PM3 calculations (Table 17). Three variables from PM3 calculations – the average polarizability E, the principal momenta of inertia around the inertial axes Y and Z (I_2 and I_3), and the relative molecular masses (M_r) and van der Waals radii (r_W) of small substituents F, Cl and CH_3 (Table 17) – showed highly significant correlations (Table 18) with lipophilicity (HPLC data; Table 9). It is important to notice the difference in the location of the centre of gravity (the intersection of the I_1, I_2 and I_3 axes) of two classes of molecules:

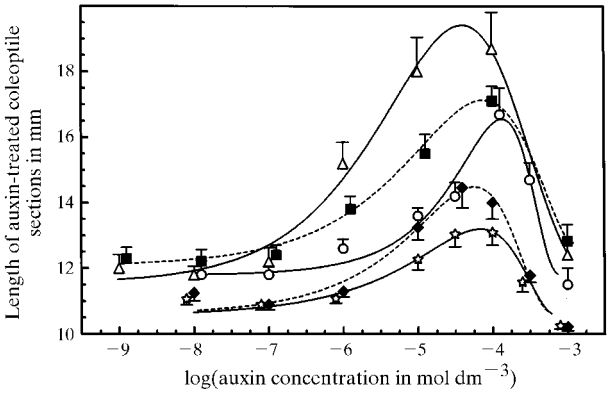

Figure 5
Sample dose–response curves obtained in *Avena* coleoptile section straight-growth bioassays for the following auxins: 5-Me-IAA (triangles, full line), IAA (squares, broken line), 2-Me-IAA (circles, full line), 5-Pr^n-IAA (diamonds, broken line) and 5-Bu^n-IAA (stars, full line). The error bars represent standard errors of the mean (n = 5–10). The dose–response curves shown are based on single experiments and are presented to illustrate the curve shapes observed with the auxins tested. Background growth (length of coleoptile sections kept in water rather than auxin solution) was ∼12 mm in the experiments with 5-Me-IAA, IAA and 2-Me-IAA, and ∼10.5 mm in the experiments with 5-Pr^n-IAA and 5-Bu^n-IAA. For quantitative comparisons, the results of replicate bioassays were corrected for background growth and averaged to yield the values shown in Table 10.

(i) indene and indole (an approximate symmetry C_{2v}) and
(ii) indole-3-acetic acid and its derivatives (C_1 molecular symmetry).

In (i) the centre of gravity is located in the plane of the aromatic ring (the axes X and Y are coplanar, and Z is perpendicular to the ring plane), whereas in (ii) it is out of the ring plane (the axes X, Y and Z intersect the ring plane at the angles $\neq 0, 90^\circ$). The results of principal component analysis (PCA) are given in Tables 18–20, and the results of principal component regression (PCR) and multiple linear regression (MLR) are presented in Table 21. In order to describe the system studied with a reduced number of independent variables and to operate in lower-dimensional space, principal component analysis is employed (Taylor & Allen, 1994; Beebe & Kowalski, 1987). In this particular case it is simpler to visualize the dataset as a three-dimensional scatterplot (Table 19, PC1–PC3) on the PC axes rather than in the more complex five-dimensional original parameter space (Table 17). PCA for the 12 molecules studied shows that they can be described well with the first two principal components (PCs) containing 90.93% of the original data (Table 17), while the first three PCs correspond to 99.41%. However, PRESS values (Table 19) suggest that the first two PCs are sufficient for the PCR. The set can be easily visualized in three dimensions (3 PCs), showing clustering (I_2, I_3) and (E, r_W), which is consistent with their large correlation coefficients (Table 18). The PC loadings (Table 20) show that for PC1 all variables are almost equally important. For PC2 M_r is less important than the others and (E, r_W) show clustering with respect to the other variables. PC3 is presented with a small contribution of I_3 and r_W.

MLR with and without the constant coefficient (Table 21) shows, according to Δ, r and other regression parameters, that lipophilicity can be represented as a linear function of five variables (E, I_2, I_3, M_r and r_W). Although there are highly correlated independent variables (I_2, I_3 and E_W, r), exclusion of only two of them resulted in poor regression. The regression vector elements (Table 21) differ much in their magnitude because the data were not autoscaled, so they do not reveal to what extent the independent variables are important for lipophilicity. PCR based on the first two PCs gives, basically, the same results as obtained in MLR without compression of data. The lipophilicity is reproduced equally well with MLR (with constant coefficient) as with PCR using all PCs. The five variables used in the regression analyses (Table 21) contribute with the same order of magnitude as revealed by the regres-

sion coefficient of PCR. The three recommended regressions (Table 21) show no significant difference in r, while MLR are preferred with respect to Δ, *sep*, F and *FIT*, but PRESS values show the opposite. The preference should be given first to PCR and then to MLR, without the constant coefficient. The *sep* and Δ values (Table 21), and the high values of r, F and *FIT* demonstrate that the regressions are satisfactory for predicting the lipophilicity of monosubstituted derivatives of IAA with small substituents attached to the benzene ring.

4. Concluding remarks

The search for a simple structure–activity correlation model valid for indole-3-acetic acid (auxin) and its alkylated and halogenated derivatives has not been a straightforward procedure. However, detailed analysis of their structural parameters and their physico-chemical properties suggests the following features of interest.

Systematic analysis of molecular structures of alkylated IAAs reveals the deviations of the phenyl moiety of the indole nucleus from the regular hexagonal symmetry (§3.1, Tables 11 and 12). This is reflected by position-specific alkylation shifts (0.06–0.29 p.p.m.) in ^{1}H NMR spectra (§3.3, Table 16). The deviation of the molecular symmetry from the ideal C_{2v} affects the momenta of inertia (I_2, I_3) as well as the average polarizability of the system. These parameters together with others (§3.6, Tables 17–21), used in QSPR, influence lipophilicity. This is corroborated by experimentally (HPLC and TLC methods) determined lipophilicities, which revealed the following general trends:

(i) 4-substituted derivatives exhibited smaller lipophilicity than the corresponding positional isomers (Table 9),

(ii) fluorine substitution at positions 5–7 of the phenyl moiety had no major effect on Π ($0.17 < \Pi < 0.19$; values determined by HPLC) and

(iii) the most lipophilic compounds are those with the substituents containing more than one C atom (Et, Pr^n and Bu^n; $0.5 < \Pi < 1.94$, Table 9).

The relatively small lipophilicity of 4-substituted IAAs can be explained by the influence of the highly hydrophilic carboxyl group in the, spatially close, 3-side chain (Fig. 1). The topological and physico-chemical characteristics of the active site of an auxin binding protein (such as ABP1) should be matched by the corresponding structural features of the substrate(s). Amongst other things, lipophilicity should be in an optimal range to fit the receptor active site. A conventional way of shifting the lipophilicity of IAA to that optimal range appears to be 4-substitution with substituents larger than F, but smaller than Et.

Except for 2-Me-IAA, all the alkyl-substituted IAAs studied here had approximately the same half-optimal and optimal concentrations, but differed with respect to the magnitude of the response. Katekar & Geissler (1982) correlated half-optimal concentrations to the affinities of the auxin receptor(s) and the maximal response to the efficacy of the auxin-receptor complex in mediating the elongation response. Thus, in terms of these authors, the affinities would be about the same for most of the compounds studied, but the efficacies depend on the size and position of the alkyl substituent. For 2-Me-IAA, which behaves differently, the receptor affinity would be 6–8 times less than for the other auxins tested. This cannot be rationalized by weak π-complexing ability and reduced NH acidity, factors otherwise used by Katekar (1979) and Thimann (1977) to explain the differences in auxin activity, because UV and ^{1}H NMR spectra (Tables 15 and 16) indicate that molecular orbital energies and charge distribution are within the same limits for all ring-alkylated IAAs. The bulk lipophilicity of 2-Me-IAA (Table 9) is also about the same as for its positional isomers. However, the polarizability E, one of five variables used in PCA to evaluate lipophilicity, was larger for 2-Me-IAA than for any of the analogues examined (Table 17). Another possible explanation for its weaker auxin activity would be steric interference of the 2-methyl group with the simultaneous recognition of the carboxyl moiety and so far not unequivocally characterized site in the pyrrole part of the indole ring system. *Ab initio* calculations (Tomić, Ramek & Kojić-Prodić, 1998) indicate that the $-CH_2COOH$ moiety in 2-Me-IAA cannot rotate as freely as in its positional isomers, which could impede the optimal orientation of the auxin molecule in the active site(s) of the auxin receptor(s). These theoretical results are supported by the experimental data on the weak binding of 2-Me-IAA to the auxin binding protein (ABP1; Rescher *et al.*, 1996).

The relative physiological activities, in *Avena* coleoptiles, for a series of substituted auxins may, in principle, be influenced by differences in transport and metabolic stability. For three of the compounds studied here (2-Me-IAA, 4-Me-IAA and 4-Et-IAA) it was, however, shown (Rescher *et al.*, 1996) that, at least in *Zea mays*, growth-promoting activity correlated well with the affinity to the most prominent endogenous auxin-binding protein (ABP1).

For the 12 indole-3-acetic derivatives examined, lipophilicity has been shown by PCA to be at most a three-dimensional phenomenon (99.41% of the variance described with the first three PCs). MLR and PCR revealed the lipophilicity to be a linear function of five variables of almost equal importance: average polarizability (E), principal momenta of inertia around inertial axes Y and Z (I_2 and I_3), relative molecular mass (M_r) and van der Waals radius (r_W) of the substitutents. These variables contain information related to the substituents F, Cl and CH_3 (their volume, shape and electronic properties), the substitution position and the conformation of the CH_2COOH moiety. Although the principal component analysis reduces the lipophilicity description to three properties (the first three PCs), the physical meaning of each of them is too complex to be identified.

This work was supported in part by the Ministry of Science and Technology, Republic of Croatia grants No 980608, 981010 and JF202 (US Croatian Research Agreement).

References

Allen, F. H. & Kennard, O. (1993). *Chem. Des. Autom. News*, **8**, 31–37.

Antolić, S., Kojić-Prodić, B., Magnus, V., Salopek, B. & Tomić, S. (1997). *Plant Physiol.* **114** (Suppl.), 158.

Antolić, S., Kojić-Prodić, B., Tomić, S., Nigović, B., Magnus, V. & Cohen, J. D. (1996). *Acta Cryst.* B**52**, 651–661.

Antolić, S., Salopek, B., Kojić-Prodić, B., Magnus, V. & Cohen, J. D. (1999). *Plant Growth Regul.* **27**, 21–31.

B. A. Frenz & Associates inc. (1982). *SDP/VAX Structure Determination Package*. College Station, Texas, USA.

Bandurski, R. S., Cohen, J. D., Slovin, J. & Reinecke, D. M. (1995). *Plant Hormones: Physiology, Biochemistry and Molecular Biology*, edited by P. Davies, pp. 38–65. Dordrecht: Kluwer Academic Publishers.

Barbier-Brygoo, H. (1995). *Crit. Rev. Plant Sci.* **14**, 1–25.

Beebe, K. R. & Kowalski, B. R. (1987). *Anal. Chem.* **59**, 1007A–1017A.

Bernstein, J., Davies, R. E., Shimoni, L. & Chang, N.-L. (1995). *Angew. Chem. Int. Ed. Engl.* **34**, 1555–1573.

Brown, R. T., Joule, J. A. & Sammes, P. G. (1979). *Comprehensive Organic Chemistry*, edited by D. Barton and W. D. Ollis, Vol. 4, edited by P. G. Sammers, pp. 411–418. Oxford: Pergamon Press.

Chandrasekhar, K. & Raghunathan, S. (1982). *Acta Cryst.* B**38**, 2534–2535.

Cleland, R. E. (1975). *Planta*, **127**, 233–242.

Cohen, D., Ginzburg, B.-Z. & Heitner-Wirguin, C. (1958). *Nature*, **181**, 686–687.

Cricket Graph 1.3 (1988). Cricket Graph Software 86/87/88, Malvern, PA.

Desiraju, G. R. (1991). *Acc. Chem. Res.* **24**, 290–296.

Dewar, M. J. S., Healy, E. F. & Yuan, Y.-C. (1990). *J. Comput. Chem.* **11**, 541–542.

Enraf–Nonius (1988). *CAD*-4 *Manual*. Version 5.0. Enraf–Nonius, Delft, The Netherlands.

Etter, M. C., Macdonald, C. & Bernstein, J. (1990). *Acta Cryst.* B**46**, 256–262.

Farrimond, J. A., Elliott, M. C. & Clack, D. W. (1978). *Nature (Lond.)* **274**, 401–402.

Fujita, T., Iwasa, J. & Hansch, C. (1964). *J. Am. Chem. Soc.* **86**, 5175–5180.

Hansch, C. & Fujita, T. (1964). *J. Am. Chem. Soc.* **86**, 1616–1626.

Hansch, C., Muir, R. M., Fujita, T., Maloney, P. P., Geiger, F. & Streich, M. (1963). *J. Am. Chem. Soc.* **85**, 2817–2824.

Hoffmann, O. L., Fox, S. W. & Bullock, M. W. (1952). *J. Biol. Chem.* **196**, 437–441.

Ilić, N., Klaić, B., Magnus, V., Vikić-Topić & Gács-Baitz, E. (1991). *Croat. Chem. Acta*, **64**, 79–88.

Johnson, C. K. (1976). *ORTEP*II. Report ORNL-5138. Oak Ridge National Laboratory, Tennessee, USA.

Karle, I. L., Britts, K. & Gum, P. (1964). *Acta Cryst.* **17**, 496–499.

Katekar, G. (1979). *Phytochemistry*, **18**, 223–233.

Katekar, G. F. & Geissler, A. F. (1982). *Phytochemistry*, **21**, 257–260.

Klämbt, D. (1990). *Plant. Mol. Biol.* **14**, 1045–1050.

Klyne, W. & Prelog, V. (1960). *Experientia*, **16**, 521–568.

Kögl, F. & Kostermans, D. G. F. R. (1935). *Hoppe Seyler's Z. Physiol. Chem.* **235**, 201–216.

Kojić-Prodić, B., Nigović, B., Tomić, S., Ilić, N., Magnus, V., Konjević, R., Giba, Z. & Duax, W. L. (1991). *Acta Cryst.* B**47**, 1010–1019.

Kowalski, B. R. & Seasholtz, M. B. (1991). *J. Chemometr.* **5**, 129–145.

Kubinyi, H. (1993). *QSAR: Hansch Analysis and Related Approaches*. Weinheim: VCH Verlagsgesellschaft.

Larsen, P. (1961). *Encyclopedia of Plant Physiology*, edited by W. Ruhland, Vol. 14, pp. 521–582. Berlin: Springer Verlag.

Leo, A., Hansch, C. & Elkins, D. (1971). *Chem. Rev.* **71**, 525–616.

Levitt, M. & Perutz, M. F. (1988). *J. Mol. Biol.* **201**, 751–754.

Libbenga, K. R., Maan, A. C., van der Linde, P. C. G. & Mennes, A. M. (1986). *Hormones, Receptors and Cellular Interactions in Plants*, edited by C. M. Chadwick and D. R. Garrod, pp. 1–68. Cambridge University Press.

Lutz, B. T. G., van der Windt, E., Kanters, J., Klämbt, D., Kojić-Prodić, B. & Ramek, M. (1996). *J. Mol. Struct.* **382**, 177–185.

Matlab 5.2. (1998). The MathWorks, Inc., Natick, MA.

Melhado, L. L., Jones, A. M., Leonard, N. J. & Vanderhoef, L. N. (1981). *Plant Physiol.* **68**, 469–475.

Mitchell, J. W. & Livingston, G. A. (1968) *Methods of Studying Plant Hormones and Growth-Regulating Substances*, Agriculture Handbook No. 336. Washington, DC: Agricultural Research Service, United States Department of Agriculture.

Muir, R. M. & Hansch, C. (1953). *Plant Physiol.* **28**, 218–232.

Muir, R. M., Hansch, C. H. & Gallup, A. H. (1949). *Plant Physiol.* **24**, 359–366.

Morales-Ríos, M. S., del Río, R. E. & Joseph-Nathan, P. (1989). *Magn. Reson. Chem.* **27**, 1039–1047.

Muñoz, M. A., Guardado, P., Hidalgo, J., Carmona, C. & Balón, M. (1992). *Tetrahedron*, **48**, 5901–5914.

Nigović, B., Kojić-Prodić, B., Antolić, S., Tomić, S., Puntarec, V. & Cohen, J. D. (1996). *Acta Cryst.* B**52**, 332–343.

Perutz, M. F. (1993). *Philos. Trans. R. Soc. Lond. Ser. A*, **345**, 105–112.

Pliška, V., Testa, B. & van de Waterbeemd, H. (1996). *Lipophilicity in Drug Action and Toxicology*. Weinheim: VCH.

Porter, W. L. & Thimann, K. V. (1965). *Phytochemistry*, **4**, 229–243.

Ramek, M., Tomić, S. & Kojić-Prodić, B. (1995). *Int. J. Quantum Chem. Quant. Biol. Symp.* **22**, 75–81.

Ramek, M., Tomić, S. & Kojić-Prodić, B. (1996). *Int. J. Quantum Chem. Quant. Biol. Symp.* **60**, 1727–1733.

Reinecke, D. M., Ozga, J. A., Ilić, N., Magnus, V. & Kojić-Prodić, B. (1999). *Plant Growth Regul.* **27**, 39–48.

Rescher, U., Walther, A., Schiebl, C. & Klämbt, D. (1996). *J. Plant Growth Regul.* **15**, 1–3.

Sachs, L. (1978). *Angewandte Statistik*. Berlin: Springer-Verlag.

Schneider, E. A. & Wightman, F. (1978). *Auxins. Phytohormones and Related Compounds — A Comprehensive Treatise*, edited by D. S. Letham, P. B. Goodwin and T. J. V. Higgins, Vol. 1, ch. 2, pp. 29–106. Amsterdam: Elsevier.

Sell, H. M., Wittwer, S. H., Rebstock, T. L. & Redemann, C. T. (1952). *Plant Physiol.* **28**, 481–487.

Sharaf, M. A., Illman, D. L. & Kowalski, B. R. (1986). *Chemometrics*. New York: John Wiley and Sons.

Sheldrick, G. M. (1976). *SHELX*76. *Program for Crystal Structure Determination*. University of Cambridge, England.

Sheldrick, G. M. (1985). *SHELX*86. *Program for the Solution of Crystal Structures.* University of Göttingen, Germany.

Spek, A. L. (1993). *PLATON. Molecular Geometry Program*. Version 1993. University of Utrecht, The Netherlands.

Starikov, E. B. & Steiner, T. (1998). *Acta Cryst.* B**54**, 94–96.

Stevens, F. J. & Su, H. F.-C. (1962). *J. Org. Chem.* **27**, 500–502.

Stewart, J. J. P. (1989*a*). *J. Comput. Chem.* **10**, 209–220.

Stewart, J. J. P. (1989*b*). *J. Comput. Chem.* **10**, 221–264.

Stewart, J. J. P. (1990*a*). *J. Comput. Chem.* **11**, 543–544.

Stewart, J. J. P. (1990*b*). *J. Comput.-Aided Mol. Des.* **4**, 1–105.

Stewart, J. J. P. (1990*c*). *MOPAC* 6.0. Frank Seiler Research Laboratory, Air Force Academy, Colorado Springs, CO.

Taylor, R. & Allen, F. H. (1994). *Sructure Correlation*, edited by H.-B. Bürgi and J. D. Dunitz, Vol. 1, pp. 111–161. Weinheim: VCH.

Taylor, R. & Kennard, O. (1982). *J. Am Chem Soc.* **104**, 5063–5070.

Thimann, K. V. (1977). *Hormone Action in the Whole Life of Plants*. Amherst: The University of Massachusetts Press.

Thomson, A., Cox, R. C. & Mansfield, T. A. (1988). *New Phytol.* **110**, 511–515.

Tian, H., Klämbt, D. & Jones, A. (1995). *J. Biol. Chem.* **270**, 26962–26969.
Tomić, S., van Duijneveldt, F. B., Kroon-Batenburg, L. M. & Kojić-Prodić, B. (1995). *Croat. Chem. Acta*, **68**, 205–214.
Tomić, S., Gabdoulline, R., Kojić-Prodić, B. & Wade, R. (1998). *J. Comp.-Aided Mol. Des.* **12**, 63–79.
Tomić, S., Ramek, M. & Kojić-Prodić, B. (1998). *Croat. Chem. Acta*, **71**, 511–525.
Venis, M. & Napier, R. M. (1995). *Crit. Rev. Plant Sci.* **14**, 27–47.
Viswamitra, M. A., Radhakrishnan, R., Bandekar, J. & Desiraju, G. R. (1993). *J. Am. Chem. Soc.* **115**, 4868–4869.